ISET Journal of Earthquake Technology, Paper No. 428, Vol. 39, No. 4, December 2002, pp. 311-346

THE STATE OF THE ART IN SEISMIC HAZARD ANALYSIS

I.D. Gupta
Central Water & Power Research Station
Khadakwasla, Pune-411024

ABSTRACT

The seismic hazard analysis is concerned with getting an estimate of the strong-motion parameters at a site for the purpose of earthquake resistant design or seismic safety assessment. For generalized applications, seismic hazard analysis can also be used to prepare macro or micro zoning maps of an area by estimating the strong-motion parameters for a closely spaced grid of sites. Two basic methodologies used for the purpose are the "deterministic" and the "probabilistic" seismic hazard analysis (PSHA) approaches. In the deterministic approach, the strong-motion parameters are estimated for the maximum credible earthquake, assumed to occur at the closest possible distance from the site of interest, without considering the likelihood of its occurrence during a specified exposure period. On the other hand, the probabilistic approach integrates the effects of all the earthquakes expected to occur at different locations during a specified life period, with the associated uncertainties and randomness taken into account. The present paper gives a critical and detailed description of both deterministic and probabilistic approaches for seismic hazard analyses. A large number of example results are presented to illustrate the implementations of the two approaches. The results of the probabilistic approach are able to account for the effects of all the controlling factors in a balanced way, and can thus be considered more reliable. The advantages quoted in favour of using the deterministic approach can simply be achieved via de-aggregation of the probabilistic hazard analysis.

KEYWORDS: Seismic Hazard, Deterministic Approach, Probabilistic Approach, Uniform Risk Spectra, Hazard De-aggregation

INTRODUCTION

The seismic hazard analysis refers to the estimation of some measure of the strong earthquake ground motion expected to occur at a selected site. This is necessary for the purpose of evolving earthquake resistant design of a new structure or for estimating the safety of an existing structure of importance, like dams, nuclear power plants, long-span bridges, high-rise buildings, etc. at that site. In earthquake engineering and related areas, it is customary to distinguish between earthquake hazard and earthquake risk, although the semantics of these two words is the same. Earthquake hazard is used to describe the severity of ground motion at a site (Anderson and Trifunac, 1977, 1978a), regardless of the consequences, while the risk refers to the consequences (Jordanovski et al., 1991, 1993). To be consistent with this terminology, in this paper, the term hazard is used to describe the ground motion and the structural response with no regard to the consequences.

By taking into account all the available database on seismicity, tectonics, geology and attenuation characteristics of the seismic waves in an area of interest, the seismic hazard analysis is used to provide an estimate of the site-specific design ground motion at the site of a structure (Dravinski et al., 1980; Westermo et al., 1980). One important application of hazard analysis is the preparation of seismic zoning maps for generalized applications (Lee and Trifunac, 1987; Trifunac, 1989a, 1990a; Anderson and Trifunac, 1977, 1978a, 1978b). By estimating the amplitudes of a parameter describing the ground motion or the earthquake effect at a closely spaced grid of sites covering the complete area of a big city or an entire state, zoning maps can be developed by contouring the sub-areas with equal hazard. Such maps find useful applications in the earthquake-resistant design of common types of structures, for which it is not possible to carry out the detailed site-specific studies. The zoning maps are also useful for land-use planning, assessing the needs for remedial measures, and estimation of possible economical losses during future earthquakes (Trifunac, 1989b; Trifunac and Todorovska, 1998).

The seismic hazard at a site can be described by a variety of parameters of ground shaking. Before the actual instrumental measurements of strong ground motion became available, various intensity scales

(MMI, MKS, etc.) based on the description of observed damages were used to describe the severity of ground motion. Intensity data are (and should be) still used as a supplement to the instrumental recordings. More recently, peak ground acceleration, and to a much lesser extent the peak velocity and displacement, had been popular instrumental measurements of ground motion. Most of the existing code provisions and design procedures have been developed in terms of peak acceleration and a normalized standard spectral shape (IAEE, 1984). However, to account for the effects of earthquake magnitude and distance on the spectral shape, one should define directly the spectral amplitudes at different frequencies by using the frequency-dependent scaling equations for the spectral amplitudes (Lee, 1987). For the seismic zoning, one should thus prepare a separate zoning map in terms of the response spectrum amplitude at each frequency (Trifunac, 1989a, 1990a). In addition, there may be other derived parameters like peak strain or liquefaction potential, for example, to quantify the seismic hazard and preparation of zoning maps (Todorovska and Trifunac, 1996a, 1996b, 1999).

There are two basic philosophies for the seismic hazard analysis, viz., deterministic and probabilistic. The former proposes design for the maximum earthquake, that is the one that will produce most severe ground motion at a site. The latter advocates that likelihood of occurrence should also be considered in view of the fact that the life of a structure is very short compared to the recurrence intervals of large events. The first basic step in seismic hazard analysis is to collect the input data on tectonics and seismicity and on ground motion scaling models. One should then decide the methodology of hazard analysis, which may be deterministic (scenario earthquake) or probabilistic (an ensemble of earthquakes). The hazard may be characterized in terms of a variety of ground motion parameters (e.g., peak amplitudes, duration of shaking, Fourier and response spectra, differential motions, artificial time histories, etc.) or the effects of ground shaking on structure (displacement, shear and bending moment envelopes) and site response (liquefaction occurrence, slope stability, permanent displacements, etc.). However, the present paper addresses mainly the issue of estimating the strong-motion parameters of interest for earthquake-resistant design and seismic safety assessment purposes.

The deterministic approach for seismic hazard analysis is not well documented in literature, and it is practised differently in different parts of the world and even in different application areas. In its most commonly used form, the deterministic method first assesses the maximum possible earthquake magnitude for each of the seismic sources (important faults or seismic provinces) within an areas of about 300 km radius around the site of a structure of interest. Then, by assuming each of these earthquakes to occur at a location that places the focus at the minimum possible distance to the site, the ground motion is predicted by using an empirical attenuation relation or some other appropriate technique.

The probabilistic seismic hazard methodology involves integrating the probabilities of experiencing a particular level of a selected strong motion parameter due to the total seismicity expected to occur in the area (about 300 km radius) of a site of interest during a specified life period (Cornell, 1968; Anderson and Trifunac, 1977, 1978a). This approach is able to consider the inherent random uncertainties and scattering present in the input database as well as in the attenuation characteristics of ground motion parameters (Lee and Trifunac, 1985; Gupta, 1991). It is thus able to provide the estimate of ground motion with a specified confidence level (probability of not exceeding). The probabilistic approach is convenient to compare risks in various parts of a country and to compare the earthquake risk with other natural and man-made hazards. For example, the design loads should be such that the risk of damage is equal throughout the country, and that it is comparable to other risks that we are prepared to take (e.g.; risk of a traffic accident, or a plane crash, or damage from floods and cyclones). The probabilistic approach opens the possibility for risk-benefit analyses and respective design motions. The motivation for such a design principle is that, at the time of construction or strengthening, if it is invested in strength beyond that required just to prevent collapse (e.g., by codes), the monetary losses during future likely earthquakes may be reduced significantly.

The strong motion parameters in both deterministic and probabilistic methodologies are commonly estimated from empirical attenuation relations in terms of earthquake magnitude, distance and soil and geologic site conditions. Where instrumentally recorded data are lacking, the scaling of strong motion parameters in terms of site intensity (e.g., Modified Mercalli) scale can also be used. Therefore, this paper first describes the attenuation and scaling relations for the peak acceleration and the response spectral amplitudes, which are the strong motion parameters used commonly to obtain the design response spectrum. The deterministic and probabilistic formulations of seismic hazard analysis are presented next. The deterministic methodology basically aims at finding the combination of the maximum possible

magnitude and the corresponding distance which would generate the highest level of ground motion at a site of interest. The probabilistic approach, on the other hand, is based on the total expected seismicity (number of earthquakes of different magnitudes) during a specified life period with its proper spatial distribution with respect to the site of interest. Various approaches to define this seismicity are reviewed briefly in the paper. Example results are presented to highlight the salient features of the probabilistic approach vis-a-vis the deterministic approach. An example of the seismic zoning via probabilistic seismic hazard analysis (PSHA) approach is also presented for the purpose of illustration.

ATTENUATION AND SCALING RELATIONS

For quantifying the seismic hazard at a site or to prepare a seismic zoning map, one needs to know the attenuation and scaling characteristics of the various strong motion parameters with distance, earthquake size and the geological conditions. Though the acceleration time-histories provide the most comprehensive description of the ground motion, due to stochastic nature of the time-history amplitudes, it is not feasible to develop the attenuation relations directly for them. Till recent past, the attenuation relations were most commonly developed for the peak ground acceleration, which was used to scale a normalized standard spectral shape (Biot, 1942; Housner, 1959; Newmark and Hall, 1969; Seed et al., 1976; Mohraz, 1976). However, this approach suffers from several drawbacks and is unable to represent various characteristics of the response spectra in a realistic way (Trifunac, 1992; Gupta, 2002). To improve upon the use of standard spectrum and peak acceleration, Trifunac and co-workers in 1977-1979 were the first investigators to develop direct scaling relations for the response spectral amplitudes at different periods. These studies were motivated by the development of similar relations earlier for the Fourier Spectrum (FS) amplitudes by Trifunac (1976). Use of such relations made it possible to incorporate in a very realistic way, the effects of earthquake size, distance, component of motion and the geological condition on the Fourier and response spectrum amplitudes and shapes. Once the response or Fourier spectrum is obtained, the design accelerograms can be synthesized to be compatible with these spectra (Tsai, 1972; Wong and Trifunac, 1979; Lee and Trifunac, 1989; Gupta and Joshi, 1993; etc.).

A large number of frequency-dependent attenuation relations have been developed by different investigators, several of which are listed in Douglas (2001). The fundamental requirements for such an attenuation relationship are that it should represent, at each frequency, the magnitude and distance saturations and the variation in geometrical spreading with distance in a realistic way. Many of the available relations do not satisfy one or the other of these requirements. The distance variation of the geometrical attenuation is neglected by most of the published relationships. Due to predominance of different types of waves at near and long distances, this variation is very important. Since mid-seventies, Trifunac and co-workers have developed several generations of the frequency-dependent attenuation relations, which have considered all of the above mentioned requirements in a very comprehensive and physically sound way. A brief review on these relations is, therefore, presented in the following.

The first generation of frequency-dependent attenuation relations due to Trifunac and co-workers were based on a uniformly processed strong motion database (Trifunac, 1977) of 186 records with a total of 558 components of motions from 57 earthquakes with $M = 3.0$ to 7.7, where M refers to M_L up to around magnitude 6.5 and to M_S for higher magnitudes. This database was first used by Trifunac (1976) to develop the attenuation relations for Fourier spectrum (FS) amplitudes at wave-periods between 0.04 and 15.0 s, in terms of earthquake magnitude M, epicentral distance R, component direction v ($v = 0$ for horizontal and 1 for vertical), and the geological condition beneath and surrounding the recording site, defined by parameter s ($s = 0$ for alluvium, 1 for intermediate and 2 for basement rock sites). Trifunac and Anderson (1977, 1978a, 1978b) developed similar relations for the absolute spectrum acceleration (SA), relative spectrum velocity (SV) and the relative pseudo spectrum velocity (PSV) for five values of damping ratio $\zeta = 0.0$, 0.02, 0.05, 0.10 and 0.20. Trifunac and Lee (1978, 1979) developed the attenuation relations for FS and PSV amplitudes with the site geological condition defined by the depth of sedimentary deposits, h (in km), rather than by the scaling parameter s.

In early 1980's, the strong motion database in California region expanded to 438 free-field records, i.e. a total of 1314 components of acceleration from 104 earthquakes. With this new database, Trifunac and Lee (1985a, 1990) developed the first frequency-dependent attenuation function, $Att(\Delta, M, T)$, as a

function of the "representative" distance Δ from the source to the site, magnitude M and period of the motion, T. Using this attenuation function, Trifunac and Lee (1985b, 1985c) presented the second generation of scaling functions for estimating FS and PSV spectral amplitudes, wherein the site geological condition was represented in terms of either s or h. These as well as the previous attenuation relations did not include the effect of local soil site condition defined by shallow alluvium and soft deposits of a few tens of meters. Therefore, using the same database of 438 records, Trifunac (1987, 1989c, 1989d) and Lee (1987, 1989, 1993) developed respectively for FS and PSV spectra, the updated attenuation relations including the effects of local soil site condition along with the geological condition on a broader scale, defined by s or h. Following Seed's (1976) classification, the local soil condition in these relations was defined by the variable s_L = 0, 1 and 2, for rock, stiff-soil and deep-soil sites, respectively.

For example, the empirical attenuation relation, when the geological condition is specified by depth of sedimentary deposits, h, is as follows (Lee, 1987):

$$\begin{aligned}\log \text{PSV}(T) = M + Att(\Delta, M, T) + b_1(T)M + b_2(T)h + b_3(T)v + b_4(T)hv \\ + b_5(T) + b_6(T)M^2 + b_7^{(1)}(T)S_L^{(1)} + b_7^{(2)}(T)S_L^{(2)}\end{aligned} \tag{1}$$

Here, $b_1(T)$ through $b_7(T)$ are the scaling coefficients, determined by regression analysis of spectral amplitudes of recorded accelerograms, for different periods and damping values, and parameters $S_L^{(1)}$ and $S_L^{(2)}$ are the indicator variables used to define the soil condition,

$$S_L^{(1)} = \begin{cases} 1 \text{ if } s_L = 1 \text{ (stiff soil)} \\ 0 \text{ otherwise} \end{cases}; \quad S_L^{(2)} = \begin{cases} 1 \text{ if } s_L = 2 \text{ (deep soil)} \\ 0 \text{ otherwise} \end{cases} \tag{2}$$

The function $Att(\Delta, M, T)$, which defines the frequency-dependent attenuation, is given by (Trifunac and Lee, 1990),

$$Att(\Delta, M, T) = \begin{cases} A_0(T)\log\Delta & ; R \le R_0 \\ A_0(T)\log\Delta - \dfrac{(R - R_0)}{200} & ; R \ge R_0 \end{cases} \tag{3}$$

with

$$A_0(T) = \begin{cases} -0.0732 & ; T \ge 1.8 \text{ s} \\ -0.767 + 0.272\log T - 0.526(\log T)^2 & ; T \le 1.8 \text{ s} \end{cases}$$

where Δ is a representative source-to-site distance, defined as

$$\Delta = S\left(\ln\frac{R^2 + H^2 + S^2}{R^2 + H^2 + S_0^2}\right)^{-\frac{1}{2}} \tag{4}$$

In this expression, R is the epicentral distance and H is the focal depth. R_0 is a transition distance (about 150 km for $T < 0.05$ s and ≈ 50 km for $T > 1$ s), and Δ_0 is the value of Δ for $R = R_0$. Function $Att(\Delta, M, T)$ depends on magnitude M implicitly through S, which is a measure of the source dimension,

$$S = 0.2 + 8.51(M - 3); \qquad M > 3 \tag{5}$$

S_0 represents the coherence radius of the source and is approximately given by $S_0 \sim \beta T/2$, where β is the shear wave velocity in the source region, and T is the wave period.

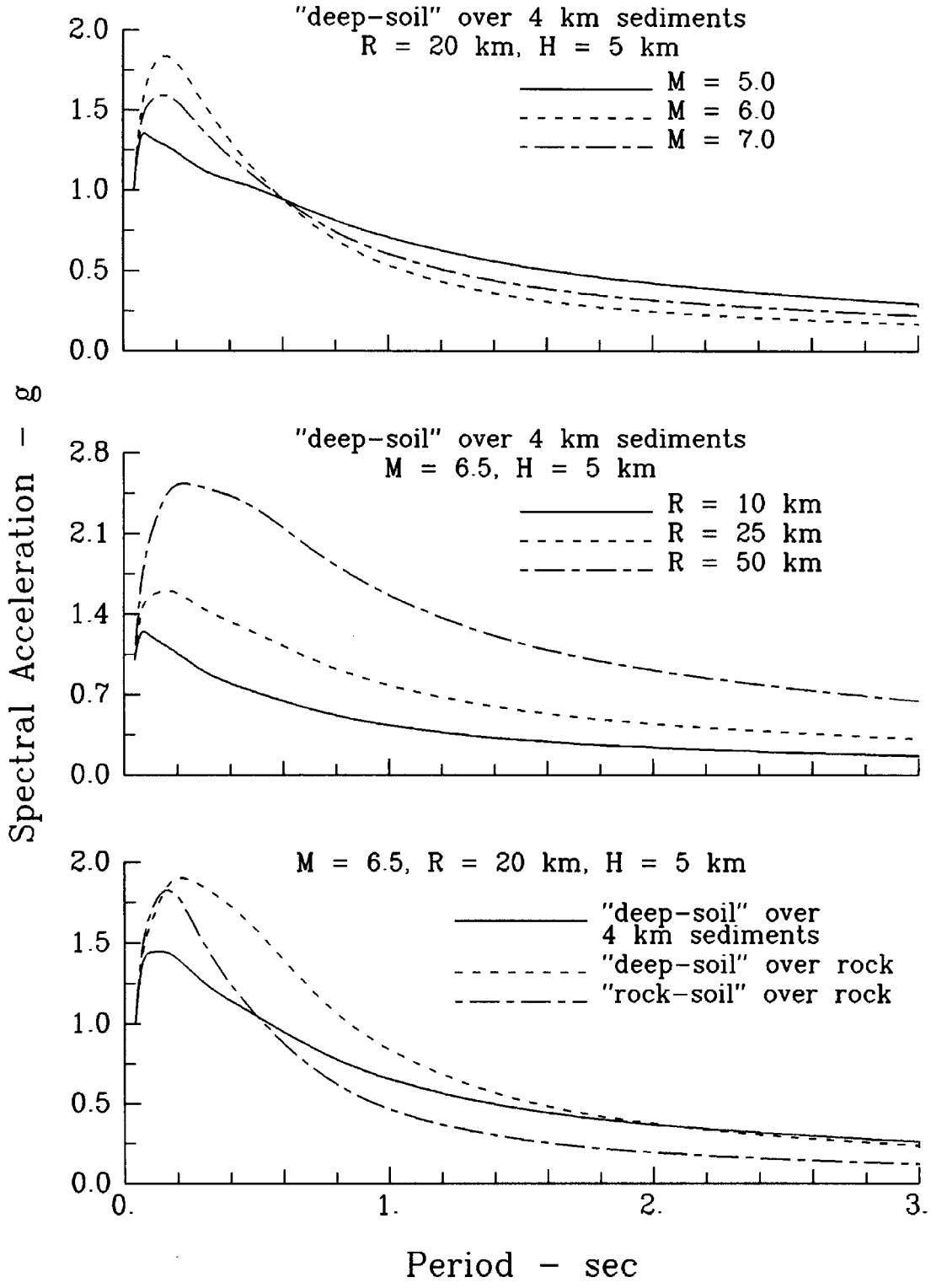

Fig. 1 Illustration of the effects of earthquake magnitude, source-to-site distance and the local soil and regional geological conditions on the normalized PSA spectra

The empirical attenuation relation, when the geological condition is defined by parameter $s = 0$, 1 and 2, is as follows (Lee, 1987):

$$\begin{aligned}\log \mathrm{PSV}(T) = {} & M + Att(\Delta, M, T) + b_1(T)M + b_2^{(1)}(T)S^{(1)} + b_2^{(2)}(T)S^{(2)} \\ & + b_3(T)v + b_4^{(1)}(T)S^{(1)}v + b_4^{(2)}(T)S^{(2)}v + b_5(T) + b_6(T)M^2 + b_7^{(1)}(T)S_L^{(1)} + b_7^{(2)}(T)S_L^{(2)}\end{aligned} \tag{6}$$

where $S^{(1)}$ and $S^{(2)}$ are the indicator variables defining the site geological condition,

$$S^{(1)} = \begin{cases} 1 \text{ if } s = 1 \text{ (intermediate geology)} \\ 0 \text{ otherwise} \end{cases}; \quad S^{(2)} = \begin{cases} 1 \text{ if } s = 2 \text{ (basement rock)} \\ 0 \text{ otherwise} \end{cases} \tag{7}$$

With $\hat{\mathrm{PSV}}(T)$ as the spectrum amplitudes estimated using Equation (1) or (6), and $\mathrm{PSV}(T)$ the spectrum amplitudes computed from recorded accelerograms, the residuals $\varepsilon(T) = \log \mathrm{PSV}(T) - \log \hat{\mathrm{PSV}}(T)$ are described by the following probability distribution

$$p(\varepsilon, T) = \left[1 - \exp\left(-\exp\left(\alpha(T)\varepsilon(T) + \beta(T)\right)\right)\right]^{n(T)} \tag{8}$$

Here, $p(\varepsilon, T)$ is the probability that $\log \mathrm{PSV}(T) - \log \hat{\mathrm{PSV}}(T) \le \varepsilon(T)$, and $\alpha(T)$, $\beta(T)$ and $n(T)$ are parameters of the distribution, which are found from a regression analysis of the observed residuals. Thus, the probability that a given spectral amplitude $\mathrm{PSV}(T)$ will be exceeded due to magnitude M at distance R is given by

$$q\left(\mathrm{PSV}(T) \mid M, R\right) = 1 - p(\varepsilon, T) \tag{9}$$

It will be shown later that this probability of exceedance is one of the basic inputs required for the probabilistic seismic hazard model.

The attenuation relations of Equations (1) and (6) can be used along with Equation (8) to evaluate the $\mathrm{PSV}(T)$ spectrum with any desired confidence level (probability of not exceeding) for given values of magnitude, distance, soil condition and regional geology, expressed in terms of depth of sedimentary deposits or qualitatively as alluvium $(s = 0)$, rock $(s = 2)$ or intermediate type $(s = 1)$. The pseudo acceleration spectrum, $\mathrm{PSA}(T)$ can be obtained from the pseudo velocity spectrum, by using the following relationship

$$\mathrm{PSA}(T) = \frac{2\pi}{T} \mathrm{PSV}(T) \tag{10}$$

Using the foregoing attenuation relations, the 5% damped pseudo acceleration spectra have been computed for various earthquake parameters and different soil and geological conditions. These spectra, normalized to an acceleration of unity at 0.04 s period, are plotted in Figures 1(a) to 1(c). Results in Figure 1(a) reveal that with increase in design earthquake magnitude, the ground motion at a site is characterized by increasing contents of long and intermediate period waves. From Figure 1(b), it is seen that with increase in source-to-site distance, the high frequency (low-period) components of ground motion are attenuated more compared to the long period components. Thus, the spectra for larger magnitudes at longer distances have relatively higher contents of intermediate and long-period motions, which is similar to the effect of alluvium and soft sedimentary deposits at the recording site. On the other hand, spectra of small magnitudes at close distances contain more of low-period waves, which is similar to the effect of hard rock condition at the recording site. Thus, to obtain realistic site specific response spectra, it is essential to consider the frequency-dependent scaling effects of earthquake magnitude and distance, in addition to that of the soil condition (Trifunac, 1990b; Gupta and Joshi, 1996). Figure 1(c) exhibits the effects of the local soil and the surrounding geological conditions on the response spectral shapes. It is seen that the spectrum on a soil site overlying directly on the basement rock or that on thick sedimentary deposits may be quite different from the spectrum on a rock site. Thus, both local soil and site geological conditions play important role in deciding the shape and amplitudes of the response spectrum at a site. The use of direct scaling relations for the spectral amplitudes provides a simple way to quantify these effects in a realistic way.

Parallel with the development of attenuation relations in terms of earthquake magnitude and distance, Trifunac and co-workers have also developed scaling relations in terms of site intensity on Modified Mercalli Intensity (MMI) scale. For areas lacking in instrumentally recorded strong-motion data, these relations may find very useful applications for seismic hazard analysis. Based on the first data set of 186 records, Trifunac (1979) and Trifunac and Anderson (1977, 1978a, 1978b) developed the scaling

relations for FS, SA, SV and PSV spectral amplitudes, with the site geological condition described by parameter s. Trifunac and Lee (1978, 1979) developed relations for FS and PSV, with geological condition in terms of the depth of sedimentary deposits, h, in km. With the expanded database of 438 records, Trifunac and Lee (1985b, 1985c) developed improved scaling relations, with geological conditions described by either parameter s or the depth of sedimentary deposits, h. Also, similar to the attenuation relations in terms of magnitude, these relations were further improved to include the effect of the local soil condition along with the geological condition of the site and the surrounding area. Trifunac (1987, 1991) developed the scaling relations for FS, and Lee (1987, 1990, 1991) for the PSV spectral amplitudes. As the expressions for both FS and PSV relations are identical, only the PSV relations are presented here as follows:

$$\begin{aligned}\log \mathrm{PSV}(T) = {} & b_1(T) I_1 + b_2(T) h + b_3(T) v + b_4(T) hv \\ & + b_5(T) + b_7^{(1)}(T) S_L^{(1)} + b_7^{(2)}(T) S_L^{(2)}\end{aligned} \tag{11}$$

and

$$\begin{aligned}\log \mathrm{PSV}(T) = {} & b_1(T) I + b_2^{(1)}(T) S^{(1)} + b_2^{(2)}(T) S^{(2)} + b_3(T) v + b_4^{(1)}(T) S^{(1)} v \\ & + b_4^{(2)}(T) S^{(2)} v + b_5(T) + b_7^{(1)}(T) S_L^{(1)} + b_7^{(2)}(T) S_L^{(2)}\end{aligned} \tag{12}$$

Various parameters in these expressions have the same meaning as described before for the attenuation relations in terms of magnitude and distance. The distributions of the residuals have been also defined in a similar way by Equation (8), which can be used to compute the spectral amplitudes with different confidence levels or to obtain the probability that a specified amplitude $\mathrm{PSV}(T)$ will be exceeded due to site intensity I_1. The site intensity due to an earthquake with epicentral intensity I_0 at distance R can also be described in a probabilistic way (Anderson, 1978; Gupta and Trifunac, 1988; Trifunac and Todorovska, 1989; Gupta et al., 1999).

DETERMINISTIC METHODOLOGY

The deterministic methodology aims at finding the maximum possible ground motion at a site by taking into account the seismotectonic setup of the area around the site and the available data on past earthquakes in the area (Krinitzsky, 1995; Romeo and Prestininzi, 2000). For this purpose, first the magnitude of the largest possible earthquake (also termed as maximum credible earthquake) is estimated for each of the seismic sources (faults or tectonic provinces) identified in an area of about 300 km radius around the site of interest. The commonly used forms of seismic sources are the line, area, dipping plane, and the volume sources. The point source is also used sometimes when the epicenters are concentrated in a very small area far away from the site of interest. The maximum magnitude in each of the sources is assumed to occur at the closest possible distance from the site. Out of all the sources, the magnitude and distance combination which gives the largest ground motion amplitude at the site is used in the deterministic method. Most commonly, the ground motion is estimated by using an empirical attenuation relation as described in the previous section. In some cases, the ground motion may also be evaluated by using empirical Green's function or stochastic seismological source model approaches (Hartzell, 1982; Hadley and Helmberger, 1980; Irikura and Muramatu, 1982; Boore and Atkinson, 1987; Gupta and Rambabu, 1996; etc.). Thus, the most important aspect of the deterministic methodology is to estimate the maximum magnitude, $M_{\max}$, for each seismic source. However, no widely accepted method exists for estimating $M_{\max}$ at present. Various methods in vogue can be grouped into two main categories: deterministic and probabilistic, which are described briefly in the following.

1. Deterministic Estimation of $M_{\max}$

The deterministic method most often used to find the maximum magnitude, $M_{\max}$, is based on the empirical regression relationships between the magnitude and various tectonic and fault rupture parameters like length, area and dislocation. Figures 2(a) and 2(b) show the relationships developed by different investigators in terms of the fault length and the fault area, respectively. It may be noted that the

sub-surface rupture length $\left(\overline{L}\right)$ can be determined more accurately from the spread of aftershock activity, and is thus considered more appropriate compared to the estimates based on surface rupture length $\left(L\right)$. The surface rupture may vary widely with geologic condition and hypocentral depth. The relationships in terms of rupture area are characterized by smaller variations compared to the rupture length relations. However, it is very difficult to predict the rupture scenario for a future earthquake, to have reliable prediction of magnitude by this method.

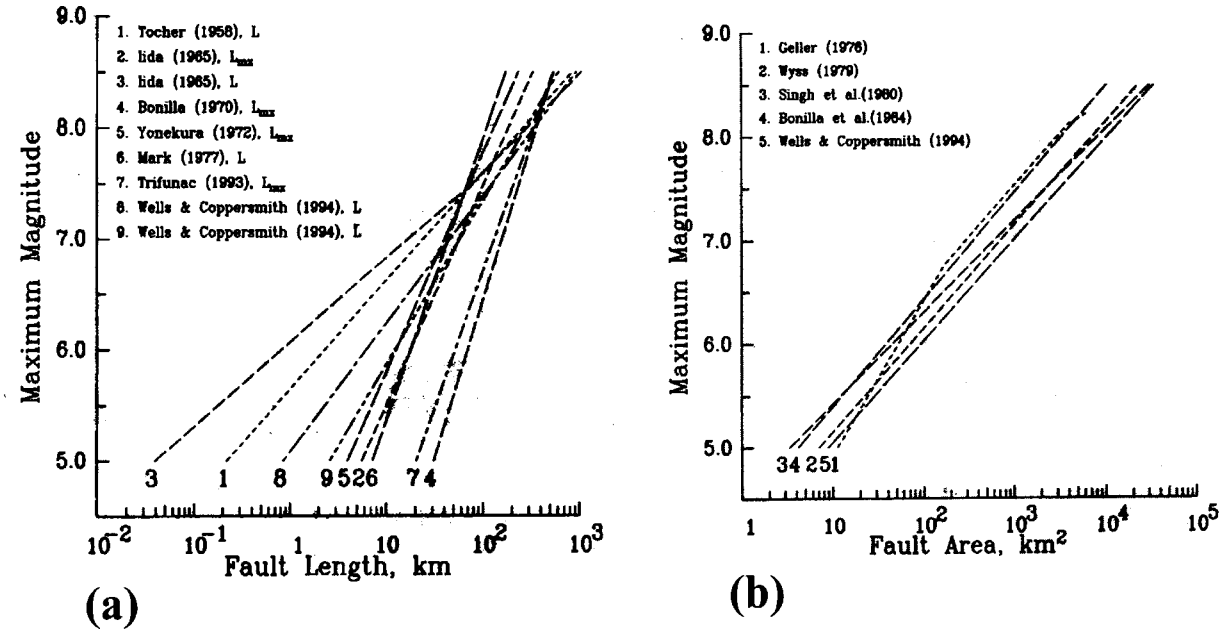

Fig. 2 Comparison of several empirical relationships used to find the maximum magnitude from (a) the fault rupture length and (b) the fault rupture area

$M_{\max}$ can also be related to the strain rate or the rate of seismic-moment release (Smith, 1976; Anderson and Luco, 1983; Papastamatiou, 1980; Wesnousky, 1986). If $M_0\left(M\right)$ is the seismic moment corresponding to a magnitude M, and $n\left(M\right)dM$ is the long-term average rate of occurrence of seismic events within a small magnitude interval of dM centered at magnitude M, the seismic moment rate $\dot{M}_0$ can be defined as

$$\dot{M}_0 = \int_{-\infty}^{\infty} M_0\left(M\right) n\left(M\right) dM \tag{13}$$

The seismic moment can be determined from earthquake magnitude using the following form of empirical relationship,

$$\log M_0 = c + dM \tag{14}$$

Hanks and Kanamori (1979) have proposed $c = 16.0$ and $d = 1.5$. The quantity $n\left(M\right)$ is an occurrence rate density function defined from the number, $N\left(M\right)$, of earthquakes per year with magnitude greater than or equal to M as

$$n\left(M\right) = -\frac{dN\left(M\right)}{dM} \tag{15}$$

Assuming that $N\left(M\right)$ can be defined by the Gutenberg-Richter's (Gutenberg and Richter, 1954) frequency-magnitude relationship truncated at the maximum magnitude $M_{\max}$, Smith (1976) has derived the following expression for estimating $M_{\max}$ from a knowledge of the moment rate $\dot{M}_0$,

$$M_{\max} = \frac{\log\left[\left(\frac{d}{d-b}\right)T\dot{M}_0\right] - c}{d} \tag{16}$$

Constant b in this expression is the slope of the Gutenberg-Richter's relationship, and this determines the proportion of large earthquakes relative to small earthquakes in a region. The term $T\dot{M}_0$ represents the cumulative moment of all the earthquakes in a time interval T, which should be the average recurrence period of $M_{\max}$. The moment rate $\dot{M}_0$ can be estimated from the geological slip rate, $\dot{u}$, and the total fault rupture area, A, as $\dot{M}_0 = \mu A\dot{u}$, where μ is the shear modulus of the rock at the fault. To use Equation (16), the recurrence interval for the maximum earthquake could approximately be estimated from the paleoseismic investigations. Though microfracturing studies of rock in laboratory and observations of earthquake sequences have led several investigators to suggest a possible relationship between b-value and seismotectonic data (Scholz, 1968; Wyss and Brune, 1968), it is not possible to estimate it from the geological data alone. It, therefore, becomes necessary to estimate this parameter from actual earthquake sequences (Esteva, 1969; Trifunac, 1994, 1998). Microearthquakes, main shocks, aftershocks, and earthquake swarms occurring within the region of interest or within geotectonically similar regions may give statistically significant estimate of b. However, the basic data on seismic slip rate (tectonic minus creep rate) may not be readily available in most cases to use this method.

To illustrate the applicability of the above method, a rough estimate of the maximum magnitude is made for the Himalayan region. From west to east, the entire Himalaya has a length of about 2500 km, and the width of the associated seismic source is about 100 km. The source of major earthquakes along the Himalaya has been postulated as a gently dipping detachment plane, north of the main boundary fault (MBF), at a depth of about 20 to 30 km (Seeber and Armbruster, 1981). Thus, the total rupture plane of the Himalaya has an area (A) of about 2.5 x 10^5 km^2. From a knowledge of the crustal model (Khattri et al., 1994), the shear modulus, μ, for the Himalayan rocks can be taken as 3.4 x 10^{11} dyne/cm^2. Also, after accounting for the trans-Himalayan deformations, the long-term average of the slip rate, $\dot{u}$, along the Himalayan detachment plane is corroborated to be only about 15 mm/year (Bilham and Gaur, 2000). This gives the moment rate $\dot{M}_0 = \mu A\dot{u}$ as 1.275 x 10^{27}dyne-cm/year. An analysis of instrumentally recorded data in the recent past suggests a b-value of about 0.9 for the Himalayan region. Thus, assuming that the recurrence period for largest earthquakes with magnitude 8(+) anywhere in the Himalaya is about 40 years, Equation (16) predicts $M_{\max}$ for such an earthquake as 8.7. This value is quite consistent with the four largest earthquakes known to have occurred in different parts of the Himalaya during the known past. However, the complete length of the Himalaya is segregated by transverse faults into independent segments not exceeding about 100 to 150 km of length. The moment rate $\dot{M}_0$ for such a segment of about 150 km would be 7.65 x 10^{25} dyne-cm/year. For $M_{\max}$ = 8.7, the expression of Equation (16) predicts an average recurrence period of about 587 years for any specified segment of the Himalaya. Thus, for the regions lacking in recorded earthquake data, information on geological slip rates, if available accurately, can be used to arrive at the maximum earthquake magnitude.

Another class of deterministic procedures is based on extrapolation of frequency-magnitude curves, derived from a short record of historical earthquakes. Though the linear extrapolation may be very conservative compared to truncated or exponential fall-off terminations (Wesnousky, 1994), it is used commonly due to lack of the exact knowledge about the non-linear nature for the large "characteristic earthquakes". Further, an extrapolation for a recurrence interval of 500 to 1000 years is used commonly, whereas the actual recurrence period may sometimes be quite different. When the available data are not adequate to define the frequency-magnitude relationship for a seismic source, the maximum earthquake magnitude is sometimes also found simply by adding an increment to the largest historical earthquake. Magnitude units of 0.5 or 1.0 are often added to get an estimate of $M_{\max}$ in many applications.

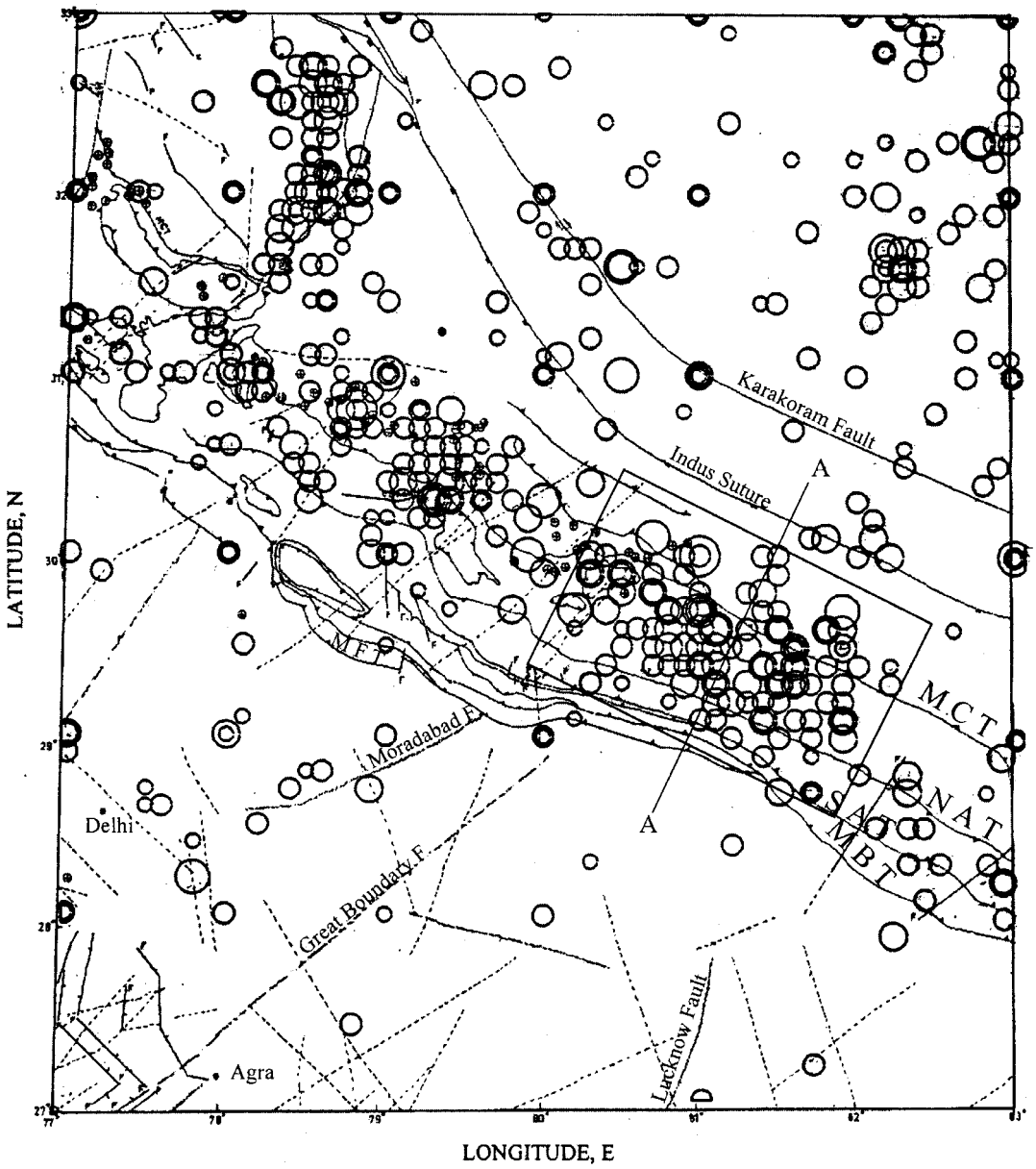

Fig. 3 Major tectonic features and the distribution of epicenters of available data on past earthquakes in a typical segment of the Himalayan region, used to compute the example results

2. Probabilistic Estimation of $M_{\max}$

The oldest probabilistic approach to find $M_{\max}$ is the use of extreme-value statistics, which was probably applied in seismology for the first time by Nordquist (1945), who used Gumbel Type-I distribution. Epstein and Lomnitz (1966) proved that the Gumbel Type-I distribution can be derived directly from the assumption that seismic events follow the Poisson distribution and the Gutenberg-Richter frequency-magnitude relationship. Use of several other extreme-value distributions has been introduced in seismology by different investigators to obtain the expected maximum magnitude for a desired return period. Gupta et al. (1988, 1994) have made a comparative study of several important extreme-value distributions and have also proposed the use of Log-Pearson Type-3 distribution for earthquake data. Such distributions have the advantage over the extrapolation of magnitude-frequency relation that they do not need data on smaller magnitudes, which are generally not reported completely for a sufficiently long time interval. The extreme-value distributions are fitted to the maximum magnitude observed per unit interval of time, commonly taken as one year. However, the available data are generally not complete even for the annual maximum magnitudes for the pre-instrumental period, and

also for the recent periods for areas with low level of seismicity and inadequate instrumentation. The estimates of the maximum magnitude from the extreme-value distributions depend on the assumed recurrence period, which may generally be associated with large uncertainty. Thus, conventionally, the extreme-value statistics does not predict M_{max} in an absolute way from a given data base.

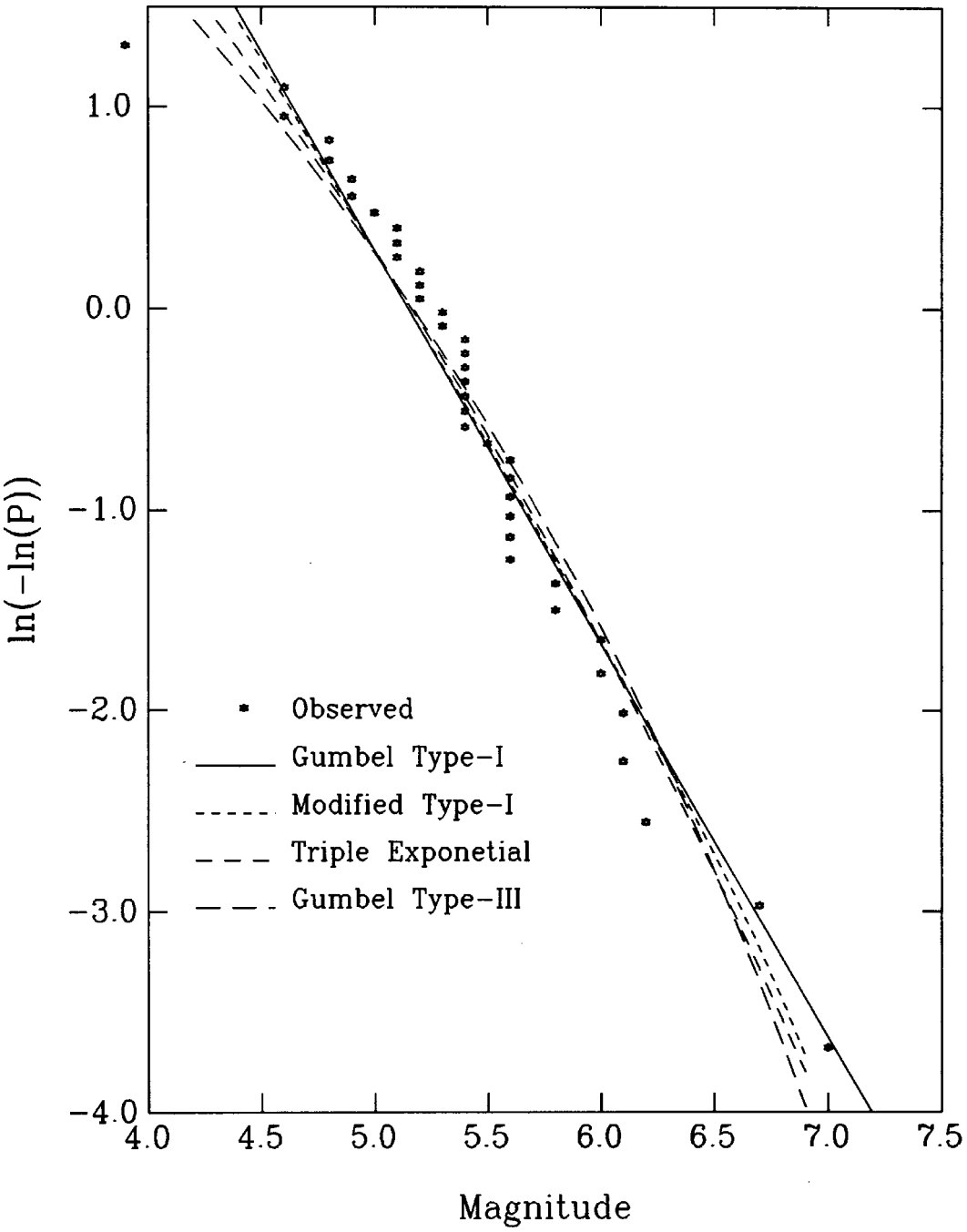

Fig. 4 Fitting of four commonly used extreme-value distributions to the available data on annual maximum magnitudes for the period 1963 to 2001 in the area of Figure 3

A more comprehensive probabilistic approach for estimating the maximum regional magnitude, M_{max}, was suggested by Kijko and Sellevoll (1989), which has been further refined recently by Kijko and Graham (1998) to consider the uncertainties in the input magnitude data. To describe the earthquake magnitude, they have used a doubly truncated exponential probability distribution function with lower cut-off magnitude M_{min}, an upper bound magnitude M_{max}, and a statistical parameter $\beta = b\ln 10$, where b is the Gutenberg-Richter's parameter. This has been then used to define the probability distribution of the maximum magnitude for a period of T years of observation. By constraining the

observed largest magnitude to be the expected value of the largest observed magnitude, Kijko (1983) has obtained an estimator for M_{max}, which requires knowledge of the mean seismic activity rate λ and the parameter β (or *b*). To estimate M_{max}, Kijko and co-workers have developed a joint maximum-likelihood function using mixed data files, consisting of an incomplete part of the earthquake catalogue containing only large historical events for a very long period and the complete part of the catalogue for a short recent period. The incomplete part is described by extreme-value distribution based on the doubly truncated magnitude distribution defined in terms of parameter β, and the complete part by the Poisson probability density function with mean occurrence rate λ. The possible standard deviations in the apparent magnitude values are accounted in these distributions by defining their Bayesian forms (Kijko and Graham, 1998). By including the expression for M_{max} into the maximum likelihood function for parameters β and λ, an iterative procedure is used to get the maximum likelihood estimate of M_{max} along with parameters β and λ.

To illustrate the application of the probabilistic method for estimation of M_{max}, a typical segment of the Himalayan region as shown in Figure 3 has been considered. The catalogue of past earthquakes for this area has been compiled for the period 1764 to 2001 from different published sources. However, to use the conventional extreme-value distribution, data on even annual maximum magnitudes is complete for a period of only 39 years from 1963 to 2001. Four different extreme-value distributions, viz., Gumbel Type-I and III (Gumbel, 1958), Modified Type-I (Chen and Lin, 1973) and Triple-exponential (Kijko and Sellevoll, 1981) distributions, are fitted to these data as shown in Figure 4. On the other hand, to apply the method of Kijko and co-workers based on a joint maximum likelihood function using mixed data files, the entire catalogue has been used. The part of the catalogue upto 1962 is treated as incomplete, which contains 17 of the largest seismic events with threshold magnitude as 5.7. The standard deviation of the magnitude for all these events is assumed to be 0.4. The subsequent part of the catalogue is considered complete and is divided into three periods as 1963 to 1971, 1972 to 1981, and 1982 to 2001, with threshold magnitudes as 5.1, 4.6 and 4.1, respectively. The corresponding uncertainties in the magnitude estimation are taken as 0.3, 0.2 and 0.2, respectively. The minimum magnitude, M_{min}, is taken as 3.8. The largest known earthquake in the area is with magnitude 7.5. Using these data, the maximum likelihood estimate $\hat{M}_{max}$ of the largest earthquake magnitude is obtained as 7.8 ± 0.57. The maximum likelihood estimates of parameters β and λ are found to be $\hat{\beta} = 2.22 \pm 0.07$ and $\hat{\lambda} = 27.05 \pm 1.59$. The expected recurrence period for the maximum magnitude is found to be 1298 years. The average values of the maximum magnitude for this recurrence period as obtained from other conventional extreme-value distributions shown in Figure 4 are: 8.8 (Gumbel Type-I), 7.6 (Modified Type-I), 7.5 (Gumbel Type-III) and 8.1 (Triple-exponential). The results of different extreme-value distributions are seen to vary widely and cannot be relied upon, because no constraint is applied to define the maximum magnitude in these distributions as has been done in the maximum-likelihood method of Kijko and co-workers.

PSHA METHODOLOGY

The results of the deterministic approach based on a single earthquake at a fixed distance from a selected site are not always able to ensure the intended conservatism for all the structures covering a wide range of frequencies. This is because the ground motion in different frequency ranges may be dominated by earthquakes of different magnitudes and distances. Thus, to get a reliable estimation of the seismic hazard at a site, it is necessary to consider the effects of all the earthquakes of different magnitudes with their proper spatial distribution around the site of interest (Cornell, 1968; Anderson and Trifunac, 1977, 1978a), and not just a single earthquake. Also, the random uncertainties in specifying the input parameters should be taken into account (Lee and Trifunac, 1985). The probabilistic seismic hazard analysis (PSHA) methodology provides a means to consider the effect of the total expected seismicity over a specified exposure period, and also the random nature of earthquake occurrences and attenuation of seismic waves with distance.

1. Theoretical Formulation

The PSHA approach is based on defining a composite probability distribution function for a selected strong-motion parameter at a site of interest due to the total expected seismicity in the area around the site during a specified exposure period. The four basic types of input to be specified and appropriately modelled for this purpose are: (i) the earthquake sources contributing to the hazard (e.g., within 300 km radius around the site), (ii) the expected total seismicity in each source, (iii) the site characteristics (e.g., geological and soil conditions), and (iv) the conditional probability that the strong motion parameter exceeds a specified level upon the occurrence of a particular earthquake. There should be a balance in the details of these inputs. The detail that significantly influences the outcome should be captured, but only if it can be obtained with reasonable accuracy and reliability. Complicated models of earthquake occurrence, which may require specification of parameters that cannot be obtained with reasonable accuracy from available data, should be avoided. The same is true for ground motion modelling; only the details that can be extracted from available strong motion data with sufficient statistical significance should be included. Another example is the modelling of geometry of the earthquake source zones. Close to the site, areal and volume zones should be used and the size of the rupture should not be neglected, while distant source zones can be modelled as line or point sources.

In actual calculations, the earthquake size is discretized, and all the earthquakes within a small magnitude interval centered around magnitude M_j are represented by M_j. The possible locations of ruptures are also discretized by distances R_i. Thus, the pair (i, j) indicates an earthquake of magnitude M_j occurring at distance R_i from the site of interest. For each such pair, the average rate of occurrence of earthquakes per year, v_{ij}, needs to be assigned. This rate depends on the rate for the entire source zone and on the probability distribution of ruptures within the zone. Then, assuming the earthquake occurrence at a location to follow the Poisson distribution, the expected number of earthquakes with magnitude M_j occurring at distance R_i from the site during a time interval of Y years is given by $n_{ij}(Y) = v_{ij}.Y$. Let X be the random variable representing a strong motion parameter (e.g., peak amplitude, spectral amplitude or site intensity), and let x be a possible level of X. Also, let $q\left(x \middle| M_j, R_i\right)$ be the conditional probability that value x will be exceeded due to an earthquake of type (i, j). The expected number of times for which $X > x$ occurs due to earthquakes of type (i, j), is equal to $q\left(x \middle| M_j, R_i\right).n_{ij}(Y)$, and the expected number of times for which $X > x$ occurs due to any type of earthquakes, is given by (Anderson and Trifunac, 1977, 1978a)

$$N_E(x) = \sum_{i=1}^{I}\sum_{j=1}^{J} q\left(x \middle| M_j,\ R_i\right).n_{ij}(Y) \tag{17}$$

The occurrence of the event $X > x$ from earthquakes of type (i, j) is a selective Poissonian process, and that from all possible earthquakes is also Poissonian (as the sum of Poissonian random variables) with parameter $N_E(x)$. Thus, the probability of $X > x$ (i.e., amplitude x is exceeded) is given by

$$P(X > x) = 1.0 - \exp\{-N_E(x)\} = 1.0 - \exp\left\{-\sum_{i=1}^{I}\sum_{j=1}^{J} q\left(x \middle| M_j, R_i\right).n_{ij}(Y)\right\} \tag{18}$$

The plots of x versus $P(X > x)$ for different exposure periods are commonly termed as "hazard curves". In many studies, the hazard curve is computed only for one year to define the annual probability of exceedance. In practical applications, the value x is determined by considering the annual probability of exceedance of the order of 1.0×10^{-5} to 1.0×10^{-3}. However, this commonly adopted practice does not provide a direct idea about the probability of exceeding value x during a specified exposure period. Therefore, in this paper, all the example results will be presented for a specified confidence level over a given exposure period.

The theoretical formulation of Equation (18) is based on the assumption that the earthquakes occur at a constant rate in time. However, it is applicable to earthquake occurrences with time-varying rate also,

provided that the total number of earthquakes, $n_{ij}(Y)$, are estimated by taking such time-dependence into account (Lee, 1992; Todorovska, 1994). Two important examples of the time-dependent activity rate are the occurrence of large characteristic earthquakes and the aftershock sequences. After a large earthquake, it takes time to accumulate the required strain energy to cause another similar earthquake at the same location (David et al., 1989). Therefore, the occurrence rate should be small soon after the occurrence of a large earthquake. However, as the elapsed time, T_o, since the previous event approaches the average return period of such an event, the occurrence rate should increase. Thus, the Poissonian model overestimates the hazard soon after the occurrence of a large earthquake, and may underestimate the hazard when the next earthquake is due or overdue. Processes of earthquake occurrence that satisfy all the Poissonian assumptions, but the one for constant rate, are of the type of "nonhomogeneous Poissonian processes". Such processes are normally specified by the hazard rate $h(t)$, which can be used to evaluate the conditional expected number of earthquakes $n_{ij}(Y|T_o)$, given the elapsed time, T_o, since the last large earthquake as

$$n_{ij}(Y|T_o) = \int_{T_o}^{T_o+Y} h(t)dt \tag{19}$$

Several investigators (Nishenko and Buland, 1987; Jara and Rosenblueth, 1988) have shown that the characteristic earthquakes along the plate boundaries can be described well by the lognormally distributed interoccurrence time period, the hazard rate for which is given by

$$h(t) = \frac{f(t)}{1 - F(t)} \tag{20}$$

Here, $f(t)$ is the lognormal density function and $F(t)$ the corresponding distribution function for the interoccurrence time *t*. These are defined as

$$f(t) = \frac{1}{\sqrt{2\pi}\zeta t} e^{-\frac{1}{2}\left(\frac{\ln t - \lambda}{\zeta}\right)^2};\ 0 \le t \le \infty \tag{21}$$

and

$$F(t) = \Phi\left(\frac{\ln t - \lambda}{\zeta}\right) \tag{22}$$

where λ and ζ are respectively the mean and standard deviation of $\ln t$, with $\Phi(\cdot)$ as the distribution function for the standard normal density function with zero mean and unit standard deviation.

The aftershock activity following a large main earthquake can be modelled as a nonhomogeneous Poisson process in time by the modified Omori's law as (Utsu, 1961)

$$n(t) = \frac{K}{(t+c)^p} \tag{23}$$

where, $n(t)$ is the rate of occurrence of aftershocks at time t after the main shock, and K, c and p are constants. Assuming the magnitude distribution to follow the Gutenberg-Richter's frequency-magnitude relationship, the occurrence rate, $\lambda(t, M_j)$, of aftershocks with magnitude M_j or greater at time t, while following a main shock of magnitude M_m, can be obtained as

$$\lambda(t, M_j) = n(t)10^{b(M_m - M_j)} \tag{24}$$

By integrating it over time and suitably distributing the resulting numbers in space, one can get the numbers n_{ij} required in the PSHA formulation.

In addition to the Poissonian occurrences, earthquakes may sometimes be postulated to occur as a result of some triggering mechanism (e.g., earth tides; Trifunac, 1970), or deterministically at certain locations in a source zone (e.g., earthquake prediction). The above probabilistic formulation can also be extended to incorporate the contributions of such events occurring in a "literal" way (Anderson and

Trifunac, 1977, 1978a; Lee and Trifunac, 1985). If $n^*_{kl}(Y)$ is the total number of such deterministic events over a time interval of Y years, the probability of $X > x$ due to these earthquakes alone is given by

$$P^*(X > x) = 1.0 - \exp\left\{\sum_{k=1}^{K}\sum_{l=1}^{L} \ln\left[1 - q\left(x \middle| M_l, R_k\right)\right] \cdot n_{kl}(Y)\right\} \tag{25}$$

The combined probability that $X > x$ from Poissonian as well as deterministic earthquakes, can be written as (Anderson and Trifunac, 1978a)

$$P^+(X > x) = 1.0 - \exp\left\{-\sum_{i=1}^{I}\sum_{j=1}^{J} q\left(x \middle| M_j, R_i\right) \cdot n_{ij}(Y)\right\} \times \exp\left\{\sum_{k=1}^{K}\sum_{l=1}^{L} \ln\left[1 - q\left(x \middle| M_l, R_k\right)\right] n_{kl}(Y)\right\} \tag{26}$$

The expression of Equation (18) or (26) can be used to compute the value, x, of a strong-motion parameter X with any desired confidence level p (probability of not exceeding). If X represents the response spectrum, $\mathrm{PSV}(T)$, or the Fourier spectrum, $\mathrm{FS}(T)$, amplitude at period T, then by computing the spectrum amplitudes at various periods with the same confidence level, it is possible to construct a complete spectrum having a constant probability of not exceeding. Such spectra were first proposed by Anderson and Trifunac (1977), and were termed as "Uniform Risk Spectra" or "Uniform Hazard Spectra". Such a spectrum has the property that it will not be exceeded with a desired confidence level, at any of the periods due to any of the earthquakes expected to occur anywhere in the region of a site of interest. Further, a uniform hazard spectrum is able to represent simultaneously and in a balanced way, the influence of the various contributing attenuation and amplification factors as well as relative contributions of all the regional earthquake sources.

Two basic input quantities required for the implementation of PSHA approach are the probability $q\left(x \middle| M_j, R_i\right)$ and the seismicity $n_{ij}(Y)$. $q\left(x \middle| M_j, R_i\right)$ defines the probability of exceeding a value x of the strong motion parameter of interest due to the magnitude and distance combination (M_j, R_i). It can be obtained from the probability distribution of the observed values of a strong-motion parameter around the expected value, as estimated from the empirical scaling relation (e.g., see Equation (9)). The seismicity $n_{ij}(Y)$ represents the total number of earthquakes expected to occur in Y years within a small magnitude range around magnitude M_j and a small distance range around distance R_i from a site of interest. This can be obtained by suitable spatial distribution of the total number, $\mathcal{N}(M_j)$, of earthquakes per year in the magnitude range M_j in each of the source zones identified in the region of the site. The evaluation of $\mathcal{N}(M_j)$ for a source zone is commonly based on fitting a magnitude recurrence relation to the available data on past earthquakes. When the data on past earthquakes is not adequate, the evaluation of seismicity can also be based on the long-term seismological slip rates. Both these approaches are described briefly in the following.

2. Evaluation of Seismicity from Past Earthquake Data

Evaluation of seismicity using available data on past earthquakes is most commonly based on the Gutenberg-Richter's (Gutenberg and Richter, 1954) recurrence relationship, according to which the yearly occurrence rate $N(M)$ of earthquakes with magnitude greater than or equal to M in a particular source zone can be described by

$$\log N(M) = a - bM \tag{27}$$

Here, a and b are constants specific to the source zone, and these can be estimated by a least square regression analysis of the past seismicity data. When the available data are not complete for a sufficiently long period of time to get statistically stable values of parameters a and b, one can also obtain these parameters from the maximum likelihood method of Kijko and co-workers, using mixed data files consisting of an extreme part for a very long historical period and the recent complete parts of the available earthquake catalogue. Once the relationship of Equation (27) has been defined for a particular

source zone, the number of earthquakes $\mathcal{N}(M_j)$ within magnitude range $(M_j - \delta M_j, M_j + \delta M_j)$ in that source zone can be obtained as

$$\mathcal{N}(M_j) = N(M_j - \delta M_j) - N(M_j + \delta M_j) \tag{28}$$

The magnitude recurrence model of earthquakes as defined by Equation (27) is quite suitable to describe the seismicity of large regions, which typically contain a number of faults. However, if it is intended to have the fault-specific sources, then it may be more appropriate to model the recurrence behaviour based on the characteristic earthquake model. In regions where repeated characteristic earthquakes have occurred during historical time, the seismicity data shows distinctly non-linear recurrence relationship (e.g., Schwartz and Coppersmith, 1984; Wesnousky, 1994; etc.). For practical applications, the earthquakes upto certain magnitude level (say, $M_{\max}$) can be defined by the exponentially decaying magnitude distribution of Equation (27) and by a uniform distribution in a narrow magnitude range (say, 0.5 magnitude unit) around the expected magnitude, M_{char}, of the characteristic earthquake (Youngs and Coppersmith, 1985). M_{char} and $M_{\max}$ may generally differ by magnitude units of 1.5 or so. As explained before, the number of characteristic earthquakes can be estimated by using Equation (19) with a lognormal density function for their interoccurrence time intervals.

The earthquake catalogues are generally incomplete for smaller magnitude earthquakes in the olden times due to inadequate instrumentation. However, due to short return periods of smaller magnitudes, their recurrence rates can be evaluated even from the most recent data for about 15-20 years. On the other hand, to get a reliable estimate for the occurrence rates of larger magnitude earthquakes with long return periods, one has to consider the data for a much longer period. Therefore, to minimize the effect of incompleteness in the available data base on the estimation of parameters a and b in Equation (27), Stepp (1973) introduced a statistical method based on the stability of the magnitude recurrence rate.

In Stepp's method, an available catalogue of earthquakes is grouped into magnitude ranges, say $\Delta M = 1$ unit, and in time intervals of about 5-10 years. The average number of events per year, $R(M)$, are then evaluated for each magnitude class for increasing time interval lengths, starting with the most recent time interval. The first window consists of the most recent years, say 5 years, the next window would consist of the recent 10 years, and so on. An analysis of the series of $R(M)$ obtained as above will show the length of the time window for which $R(M)$ becomes stationary for a given magnitude range. Thus, Stepp's method involves determining that fraction of the total time sample, in which the mean rate of occurrence, $R(M)$, is stable for each magnitude class. For this purpose, $R(M)$ is modelled as a Poisson point process in time, such that the standard deviation of $R(M)$ for a time interval of T years is given by

$$S_R = \sqrt{R(M)/T} \tag{29}$$

Assuming stationarity of $R(M)$, S_R will behave as $1/\sqrt{T}$. The plot of the standard deviation S_R as a function of T is known as the "completeness plot". For a particular magnitude class, the period of completeness is reflected in this plot by a distinct departure of the S_R values from the linearity of the $1/\sqrt{T}$ slope. This period, which should be a minimum for a stable $R(M)$, becomes successively longer with each higher magnitude class. A typical completeness plot for the available earthquake data for the region of Figure 3 is shown in Figure 5. Thus, to fit the relationship of Equation (27), the annual number of earthquakes in a particular magnitude range can be found by using the data for the period for which that magnitude range is recorded completely.

To consider the spatial distribution of the seismicity within a source zone, the entire source zone is divided into a large number of small source elements. The center of each of these elements is the possible location of earthquakes. Depending on the position of the element with respect to the zone boundaries, likelihood can be assigned that an earthquake of given size occurs in that element (e.g., larger magnitude earthquakes are less likely to initiate close to the zone boundary). On the basis of such likelihood, the

number $\mathcal{N}(M_j)$ for the source zone can be distributed among the source elements, to get the expected number, $n_{ij}(Y)$, of earthquakes of size M_j in the ith source element.

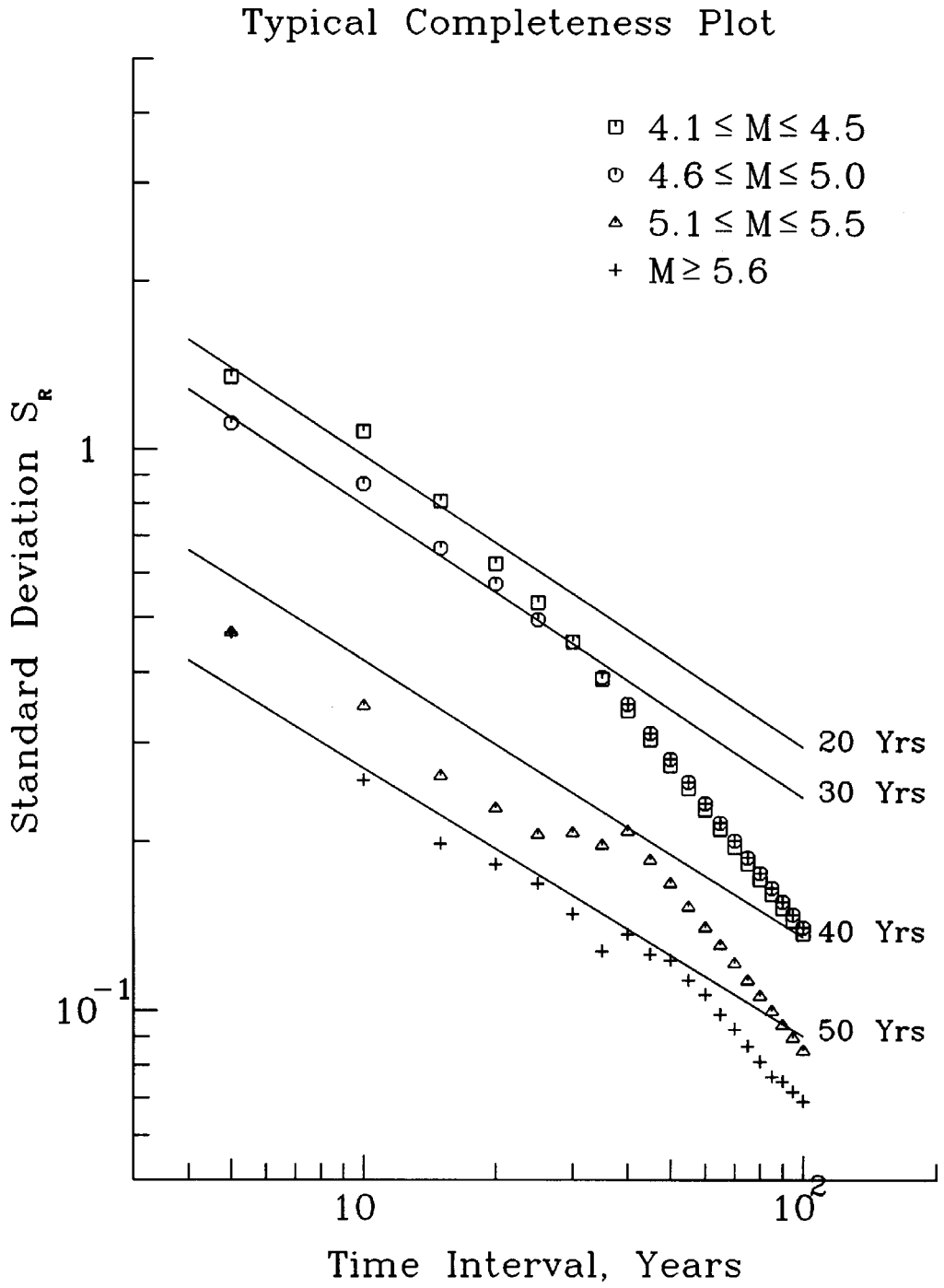

Fig. 5 A typical completeness plot for the available data on past earthquakes in the area of Figure 3 (the most recent time intervals for which different magnitude classes are recorded completely are also indicated in the figure)

3. Evaluation of Seismicity from Geological Data

The theoretical background used to develop the expression of Equation (16) to estimate the maximum magnitude, $M_{\max}$, from the moment rate can also be used to define a frequency-magnitude relationship, if $M_{\max}$ is assumed to be known. To illustrate this, the Gutenberg-Richter's recurrence relation, with upper bound magnitude as $M_{\max}$, can be written as

$$N(M) = K_0 10^a \left(10^{-bM} - 10^{-bM_{\max}}\right);\ K_0 = \left(1 - 10^{-bM_{\max}}\right)^{-1} \tag{30}$$

This gives the occurrence rate density function $n(M)$ as

$$n(M) = -\frac{dN(M)}{dM} = K_0 b 10^{a-bM} \ln 10 \tag{31}$$

Using this and $M_0(M)$ defined by Equation (14) in Equation (13), and performing the integration, one gets

$$\dot{M}_0(M) = \frac{K_0 b}{d-b} 10^a \left[M_0(M_{\max}) 10^{-bM_{\max}} - 10^c\right] \tag{32}$$

Substituting the value of 10^a from this expression into Equation (30) gives the mean occurrence rate for magnitudes greater than or equal to M as

$$N(M) = \frac{\dot{M}_0(d-b)}{b} \cdot \frac{10^{b(M_{\max}-M)} - 1}{M_0(M_{\max}) - 10^{c+bM_{\max}}} \tag{33}$$

Even for very small values of $M_{\max}$ (say, about 5.0), this expression can be simplified, without any significant effect on the final results, as follows:

$$N(M) = \frac{\dot{M}_0(d-b)}{b} \cdot \frac{10^{b(M_{\max}-M)}}{M_0(M_{\max})} \tag{34}$$

If, in addition, N_C number of characteristic earthquakes with magnitudes distributed uniformly in the interval $(M_{\text{char}} - \Delta M_{\text{char}}/2,\ M_{\text{char}} + \Delta M_{\text{char}}/2)$ also contribute to the moment release rate, $\dot{M}_0$ in this expression has to be replaced by $\dot{M}_0^{\text{char}}$, defined as

$$\dot{M}_0^{\text{char}} = \dot{M}_0 - \frac{N_C}{\Delta M_{\text{char}}} \cdot \frac{M_0(M_{\text{char}})}{d \ln 10} \left[10^{d\Delta M_{\text{char}}/2} - 10^{-d\Delta M_{\text{char}}/2}\right] \tag{35}$$

As described before for the estimation of $M_{\max}$, the moment rate $\dot{M}_0$ in the above expressions can be obtained from the total fault area (A), and the long term average of geological slip rate, $(\dot{u})$, as $\dot{M}_0 = \mu A \dot{u}$. However, parameter b has to be estimated from the available seismological data for the region of interest or another region with similar seismotectonic setup. Thus, the foregoing formulation can be used for evaluating the seismicity from the geologically determined slip rate. Slip-rate data is generally available for major faults in a region. These rates are primarily established from offsets of geological formations or geomorphic features (e.g., offsets of terraces and stream courses) along the faults and through detailed study of creep rates, trenching and age dating. Slip rates may also be determined from available geodetic measurements.

To illustrate the application of the above formulation for estimation of seismicity, let us consider a 150 km long segment of the Himalayan arc. The source of major earthquakes along this segment can be considered a gently dipping detachment plane of about 100 km width. Taking μ = 3.4 x 10^{11} dyne/cm^2 and $\dot{u}$ = 15 mm/year, as explained before, one gets $\dot{M} = \mu A \dot{u}$ = 7.65 x 10^{25} dyne-cm/year. For $M_{\max}$ as 8.0 and b as 0.9, Equation (34) then leads to the following frequency-magnitude relationship:

$$\log N(M) = 4.9 - 0.9M \tag{36}$$

This relation can be reconciled very well with the available data on past seismicity in different parts of the Himalaya. Thus, the information on geological slip rates can be used to obtain the earthquake recurrence relations for estimating the seismicity for the purpose of seismic hazard analysis.

UNCERTAINTIES IN SEISMIC HAZARD ANALYSIS

The foregoing PSHA formulation has accounted for the uncertainties related to the inherent random nature of the various input parameters used to describe the seismicity and the ground motion attenuation. For example, the random nature of earthquake recurrence is described by Poisson model, that of earthquake magnitudes by Gutenberg-Richter's relation, that of earthquake location by spatial distribution of the total number of earthquakes in a source zone, and that of the ground motion attenuation by the probability distribution about the mean attenuation law. Such random nature of the input parameters is commonly termed as the "aleatory" uncertainties, which are inherent to the physical processes generating the seismicity and the ground motion. These uncertainties cannot be thus eliminated completely, though it may be possible to minimize them by collecting more and good quality of data.

Further, the parameters describing the aleatory uncertainties may themselves be associated with some uncertainties due to limited amount of the available data used for their estimation. It is therefore necessary to describe these parameters by suitable probability distributions and to replace them by their Bayesian estimates. For example, if the parameters a and b in the Gutenberg-Richter's relationship are described respectively by probability density functions $f(a)$ and $f(b)$, the Bayesian estimate, $\hat{N}(M_j)$, of the number of earthquakes with magnitude M_j or more can be defined as

$$\hat{N}(M_j) = \int_{-\infty}^{\infty}\int_{-\infty}^{\infty} N(M_j|a,b) f(a) g(b) da db \tag{37}$$

Here, $N(M_j|a,b)$ is the number of earthquakes obtained from Equation (27) for specified values of parameters a and b. If μ_a and μ_b are the mean values and σ_a and σ_b the corresponding standard deviations of parameters a and b, then on assuming both a and b to follow the Gaussian probability distribution, the integral in Equation (37) can be evaluated to get

$$\hat{N}(M_j) = N(M_j) 10^{\frac{1}{2}\left(\sigma_a^2 + \sigma_b^2 M_j^2\right)\ln 10} \tag{38}$$

where $N(M_j)$ is the number of earthquakes obtained from Equation (27) by using mean values of a and b. Further, the upper-bound cut-off magnitude, $M_{\max}$, is also generally associated with large uncertainty, which can be described via some probability density function over the expected range of $M_{\max}$ (Lee and Trifunac, 1985). Thus, the expected number of earthquakes within magnitude interval $(M_j - \delta M_j, M_j + \delta M_j)$, with a, b and $M_{\max}$ all taken as random, can be estimated by multiplying $\hat{N}(M_j)$ obtained from Equation (38) with the probability that $M_j \le M_{\max}$, evaluated by assuming a probability density function for $M_{\max}$.

In addition to above, both probabilistic and deterministic approaches are subject to the uncertainties in modelling the seismic sources, seismic activity of each source, and the attenuation of strong motion parameters in an exact way (Abrahamson, 2000; Stepp and Wong, 2001). The seismic activity of a source zone refers to the maximum magnitude and its distance from a selected site in case of the deterministic approach, and the total seismicity for a specified time period with spatial distribution over the entire source zone in case of the PSHA approach. The modelling uncertainties are commonly termed as "epistemic" uncertainties, which are associated mainly with the lack of exact knowledge of the physical processes. Thus, at least in principle, it is possible to eliminate these uncertainties by collecting more data to arrive at the exact models for the seismic sources and the ground motion attenuation laws.

In the deterministic approach, the epistemic uncertainties may generally lead to several possible alternatives for the maximum credible earthquake magnitude, its source-to-site distance from the site of interest, and the ground motion attenuation relation, which in turn would lead to several different estimates of the ground motion. The effects of these uncertainties can be accounted for by defining a discrete probability density function for all the alternatives and by estimating the "mean" or "median" value of the ground motion parameter. In the PSHA approach, the "logic-tree" formulation is often used to incorporate the effects of both aleatory and epistemic uncertainties (Coppersmith and Youngs, 1986; SSHAC, 1997; Savy et al., 2002). The logic-tree methodology considers a large number of different

probabilistic models and model parameters, and computes the hazard for all the combinations of parameter values defined by the end branches of the logic-tree. Each of the input parameters is assigned an appropriate weight to define a discrete probability density function for the frequency, $N_E(x)$, of exceeding a value x of a strong motion parameter X, as defined by Equation (17). One can then obtain the various statistical estimates of the frequency of exceeding x; the most common among them is the expected (mean) value, defined as

$$\bar{N}_E(x) = \sum_{\theta_k} N_E(x|\theta_k) p(\theta_k) \tag{39}$$

where, $p(\theta_k)$ represents the discrete probability density function for the parameter set θ_k. The use of the hazard curve based on $\bar{N}_E(x)$ is able to consider the effect of all the uncertainties in the probabilistic estimation of the seismic hazard.

DE-AGGREGATION OF PROBABILISTIC SEISMIC HAZARD

The probabilistic seismic hazard analysis (PSHA) carries out integration over the total expected seismicity during a given exposure period to provide the estimate of a strong-motion parameter of interest with a specified confidence level. The PSHA is thus able to quantify and account for the random uncertainties associated with estimation of the seismicity and the attenuation characteristics of the region. However, the physical image of an earthquake in terms of magnitude and source-to-site distance is lost in the PSHA analysis. For physical interpretation of the results from PSHA and to take certain engineering decisions, it is desirable to have a representative earthquake which is compatible with the results of the PSHA method (Trifunac, 1989b). This could be achieved through the de-aggregation of the probabilistic seismic hazard, as described in the following (McGuire, 1995).

The basis of the PSHA methodology is the expression of Equation (19), which defines for a site of interest the probability of exceeding a value x of a selected strong-motion parameter X, due to the total expected seismicity in the area around the site during a specified exposure period. The seismicity refers to the number, $n_{ij}(Y)$, of earthquakes with magnitude M_j occurring at distance R_i. From Equation (18), one can estimate the value of the strong motion parameter X with a specified probability of exceedance p. If this value is represented by x_p, the de-aggregation of PSHA aims at finding the relative contribution of the earthquakes of type (i, j) to the probability of $X > x_p$. This is the same as the conditional probability of M_j and R_i, given that $X > x_p$, which can be defined as

$$f(M_j, R_i | X > x_p) = \frac{1.0 - \exp\{-q(x_p | M_j, R_i) n_{ij}(Y)\}}{1.0 - \exp\{-\sum_{i=1}^{I}\sum_{j=1}^{J} q(x_p | M_j, R_i) n_{ij}(Y)\}} \tag{40}$$

The numerator on the right hand side of this expression represents the probability of $X > x_p$ due to earthquakes of type (i, j), and the denominator represents the probability of $X > x_p$ due to all the expected earthquakes. The representative values of earthquake magnitude and distance can be obtained from this distribution as

$$\overline{M} = \sum_{i=1}^{I}\sum_{j=1}^{J} M_j f(M_j, R_i | X > x_p) \quad \text{and} \quad \overline{R} = \sum_{i=1}^{I}\sum_{j=1}^{J} R_i f(M_j, R_i | X > x_p) \tag{41}$$

The value of the strong-motion parameter X with probability of exceedance p, as obtained using these values of magnitude and distance, will be matching closely with the value x_p as obtained by the PSHA approach. $\overline{M}$ and $\overline{R}$ may thus be termed as hazard-consistent magnitude and distance, respectively (Ishikawa and Kameda, 1988; Kameda, 1994).

In principle, PSHA can be performed for any of the strong motion parameters. However, in practice, it is more often carried out for the peak ground acceleration and the response spectral amplitudes only.

Thus, the hazard-consistent magnitude and distance may be very handy for selecting ground motion characteristics like duration, nonstationarity, etc. for the purpose of generating spectrum-compatible design accelerograms. However, one basic problem with the de-aggregation of PSHA stems from the fact that to reproduce the amplitudes of a uniform hazard spectrum at different natural periods, the hazard-consistent magnitude and distance are found to vary significantly. Thus, in general, it is not possible to define a single representative earthquake, which can be consistent with an entire uniform hazard spectrum (Trifunac, 1989b).

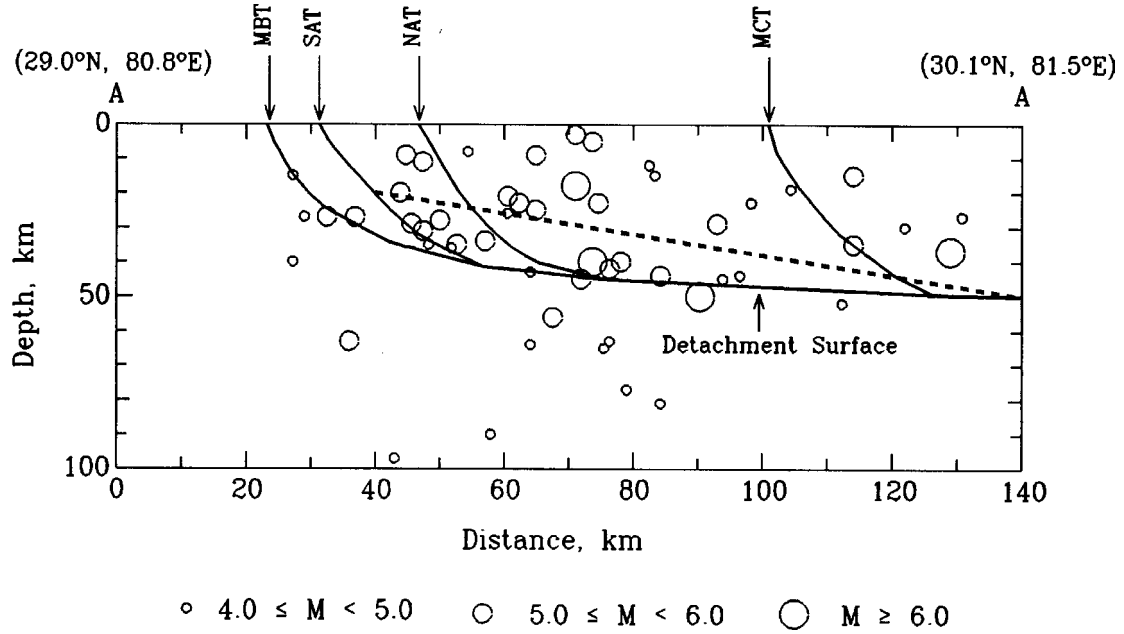

Fig. 6 The depth section along line A-A in Figure 3 of the available data on past earthquakes in an area of about 150 km long segment of the Himalayan arc (the possible location of the postulated Himalayan detachment plane is also shown in the figure)

EXAMPLE RESULTS

To illustrate how the results of probabilistic seismic hazard analysis (PSHA) are able to account for, in a realistic way, the effects of various seismotectonic and geological parameters, a 150 km long segment of the Himalayan arc around line A-A in Figure 3 has been considered as the seismic source. The depth section of the available past earthquake data in this source is shown in Figure 6. As mentioned before, major earthquakes in the Himalaya are associated with a gently dipping detachment surface north of the main boundary thrust (MBT) to which the various Himalayan thrusts join at steep angles (Seeber and Armbruster, 1981). The other thrusts north of MBT along section A-A in Figure 3 are the South Almora Thrust (SAT), North Almora Thrust (NAT) and the Main Central Thrust (MCT). It is seen that earthquakes with magnitude greater than or equal to 6.0 are mostly associated with the detachment surface as shown in Figure 6, whereas more of smaller magnitudes occur at shallower depths. Also, it is seen that there is a general decreasing trend in the number of earthquakes as one goes to the north from MBT. The example seismic source, which is about 150 km long and 100 km wide area of the crustal detachment surface along the Himalaya, has been idealized by a detachment plane, as shown in Figure 6 by a dashed line. A three-dimensional schematic of this seismic source is depicted in Figure 7.

The example results are computed in the form of pseudo acceleration spectra (PSA) with a damping ratio of 5%, by using the attenuation relations due to Lee (1987). To define the average seismicity of the above source, the moment rate $\dot{M}_o$ is taken as 1.0 x 10^{26} dyne-cm/year, $M_{\max}$ as 8.0, and the $b-$value as 0.9. The exposure time for estimating the total seismicity is taken as 100 years. From Equation (34), the Gutenberg-Richter's productivity coefficient a for these values works out to be 5.0. For the present computations, the lower threshold magnitude has been taken as 4.0, because smaller magnitudes are not expected to be of much engineering significance. To evaluate the total expected number of earthquakes $\mathcal{N}\left(M_j\right)$ in different magnitude intervals $\left(M_j-\delta M_j, M_j+\delta M_j\right)$, the magnitudes between the

minimum and the maximum values are discretized with interval $\delta M_j = 0.25$. To consider the spatial distribution of seismicity, numbers $\mathcal{N}\left(M_j\right)$ are distributed all over the surface projection of the detachment plane. For this purpose, the entire surface area is divided into small elements of 5 km x 5 km size as shown in Figure 7, and the epicenters are assumed to occur at the centers of these elements. In view of the observed spatial distribution of the past earthquakes, the probability of earthquake occurrences is assumed to decrease linearly to one half as one goes from the southern boundary to the northern boundary of the seismic source. The focal depth of earthquakes with magnitude 6.0 or more is taken as the depth of the detachment plane, whereas those with smaller magnitudes is assumed to be 10 km shallower. Thus, the presented example can be considered to represent a generalized situation for a 150 km long typical segment anywhere along the Himalaya. However, as the attenuation relations used are not specific to the Himalayan region, the conclusions drawn are to be considered of qualitative nature only.

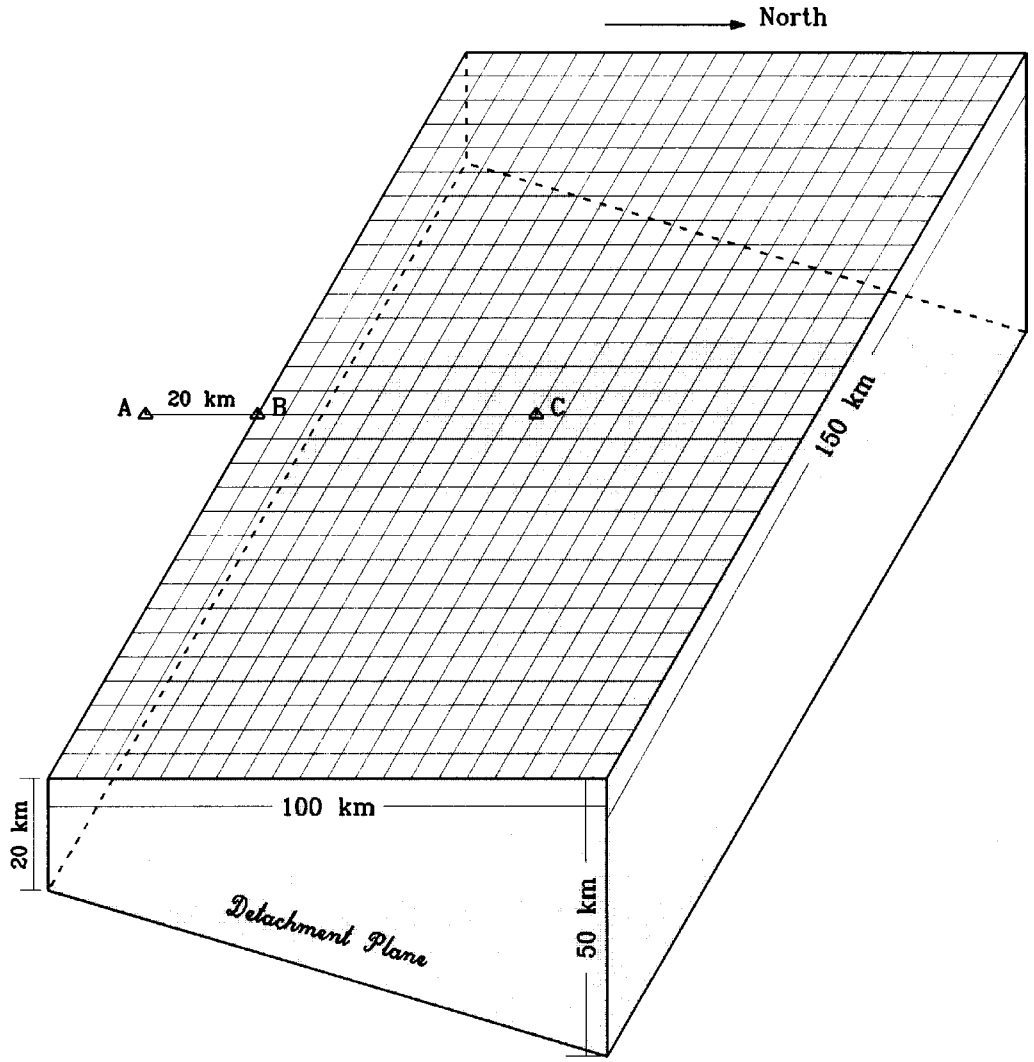

Fig. 7 An idealized schematic diagram of the seismic source (a detachment plane) indicated in Figure 6 by dashed line (example results are computed by discretizing the surface projection of the source plane into rectangular elements of 5 km x 5 km size)

First of all, to study the effect of the confidence level on the uniform hazard response spectrum, example results are computed for three different confidence levels of 0.1, 0.5 and 0.9 for site-A in Figure 7 at a distance of 20 km from the surface projection of the seismic source. To illustrate how the results of the deterministic approach compare with the results of PSHA approach, corresponding response spectra are also obtained for $M_{\max} = 8.0$ with focal depth of 20 km and distance as 20 km from site-A. Both these spectra are shown plotted in Figure 8, from which it may be inferred that, in general, it would not be

possible for any pair of M_{max} and its distance to match the results of the deterministic approach with those of the PSHA approach over the entire period range and for all the confidence levels. In the presented example, the PSHA spectra show narrower probability distribution, which is also seen to be shifted towards higher amplitudes. Thus, the common belief that deterministic approach is always more conservative is not true in general.

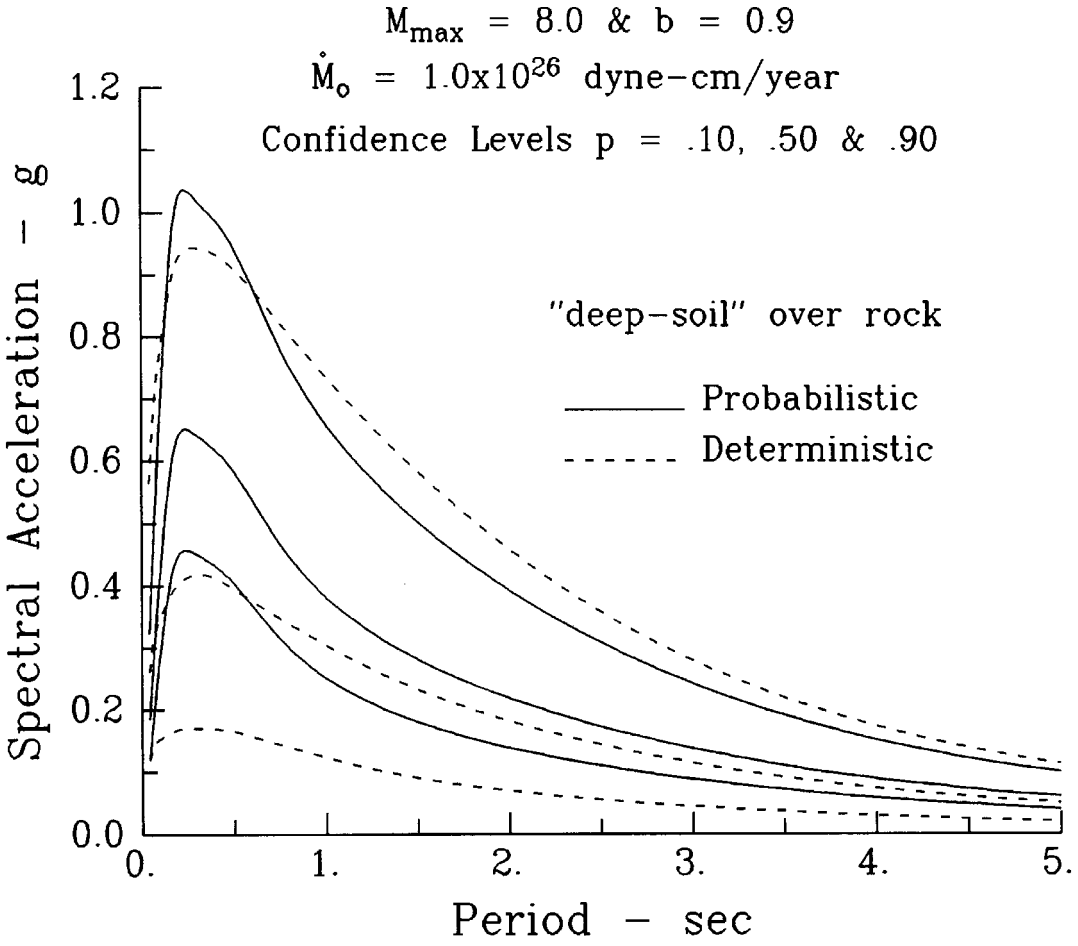

Fig. 8 Comparison of the response spectra of horizontal component of motion obtained by the PSHA and deterministic approaches for different confidence levels

Figure 9 shows the comparison between the probabilistic and deterministic spectra with a confidence level of 0.5 for the horizontal and vertical components of motion. For both the components, the spectra of PSHA approach are seen to be significantly higher in almost the entire period range. From the results in Figure 9, it is further observed that for deep-soil sites overlying the basement rock, the spectral amplitudes for vertical motion are comparable with the horizontal motion for periods greater than about 3.5 s. The conformity between the deterministic and the probabilistic spectra in this regard confirms the fact that the probabilistic spectra are able to take into account in a physical way the dependence on the various governing parameters. To illustrate further the physical nature of the PSHA approach, Figures 10 and 11 show the influence of the local soil condition and the depth of sediments underneath on the uniform hazard spectra. Figure 10 shows the spectra for "rock-soil" over rock and "deep-soil" over rock, where the latter parameter refers to geological basement rock (i.e., no sediments). Taking the "rock-soil" and rock as reference, it is seen that at longer periods, "deep-soil" amplifies the spectral amplitude, and at smaller periods, it attenuates the amplitudes. In most cases, "rock-soil" is found over rock and "deep-soil" over thick sediments. Uniform hazard spectra for these extreme conditions are shown in Figure 11. It is seen that at longer periods, the sediments further amplify the spectral amplitudes, whereas the amplitudes are practically same for smaller periods. Thus, compared to "deep-soil" over rock, the sediments also amplify the low-period amplitudes. It is thus established that the PSHA methodology is able to represent in a physically realistic way the influence of both the local soil and the surrounding geological condition.

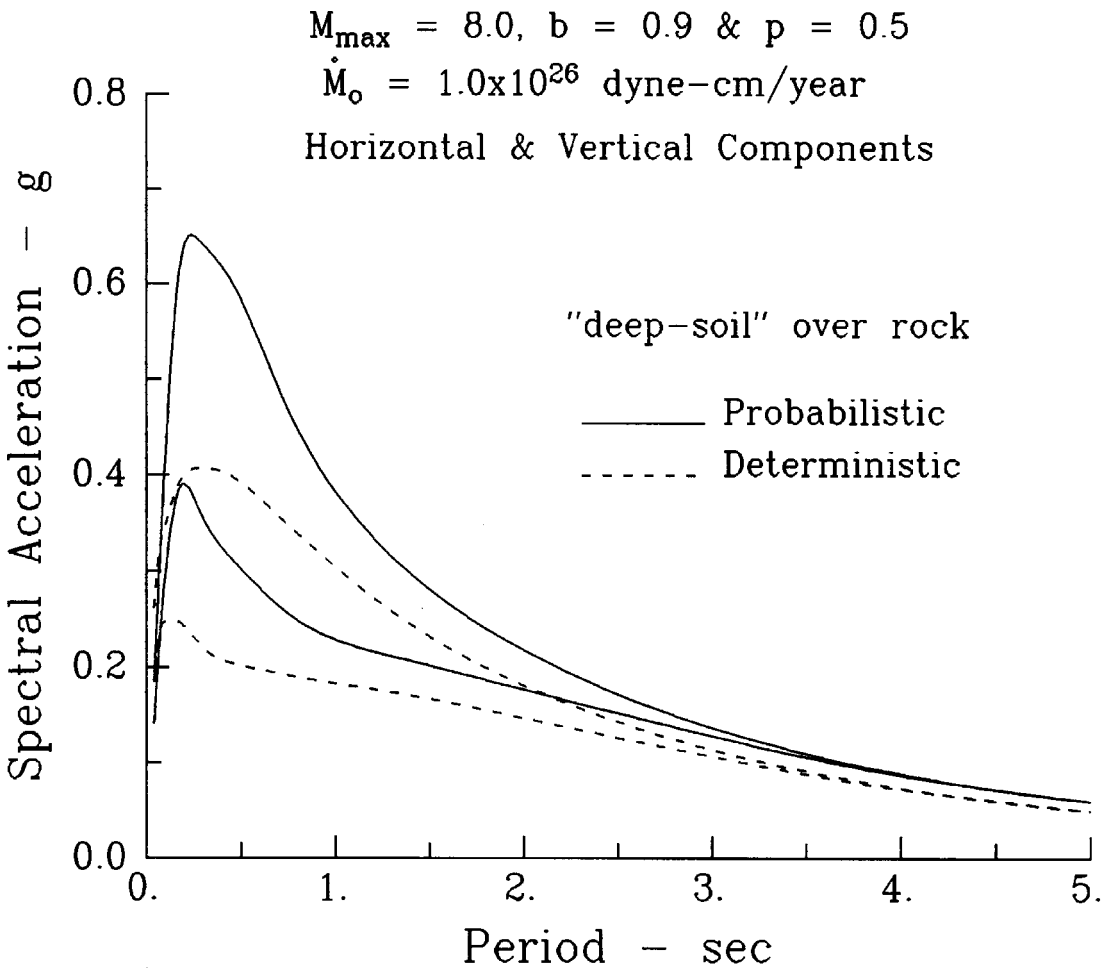

Fig. 9 Comparison of the response spectra obtained by the PSHA and deterministic approaches for the horizontal and vertical components of motion with a confidence level of 0.5

Next, to illustrate the effect of the spatial distribution of seismicity with respect to the site of interest, uniform hazard spectra are computed for three sites indicated by solid triangles A, B and C in Figure 7. Site-A is located at a distance of 20 km from the center of the southern boundary of the surface projection of the seismic source, site-B is located at the center of this boundary, and site-C lies at the center of the area of the surface projection. Thus, for sites-A to C, the distance from the seismic source is decreasing continuously. As described before, the spatial distribution of the seismicity is considered to be non-uniform in such a way that the probability of earthquake occurrences reduces linearly to one-half, as one goes from the southern boundary to the northern boundary of the seismic source. The focal depths for earthquakes with magnitudes greater than or equal to 6.0 are taken as the depth of the detachment plane shown in Figure 7, and those with smaller magnitudes as 10 km shallower. In addition, for the purpose of comparison, results are also computed for a uniform spatial distribution of the seismicity with a constant focal depth of 20 km for all the earthquakes. Both these results are presented in Figure 12, where thick curves correspond to the non-uniform and thin curves to the uniform distribution of the seismicity. It is seen that at the same site, the shape and the amplitudes of the uniform hazard spectrum may differ significantly with change in the spatial distribution of the seismicity. For the case of uniform distribution of seismicity, with decrease in the distance, the spectral amplitudes are seen to increase over the entire period range. However, this increase is not same at all the periods. On the other hand, for non-uniform distribution of seismicity, the variation in the response spectral amplitude is seen to be quite typical. For example, the response spectrum at site-B is higher over the entire period range than that at site-C, though site-C is closer to the seismic source.

The PSHA approach can also be used to prepare the seismic zoning maps for an area. Seismic zoning can be done on a macro or a micro scale, depending on the size of the area (a whole region or a whole country versus a metropolitan area, for example). The strong-motion parameters used for seismic zoning may also vary widely, such as the Modified Mercalli Intensity (Gupta et al., 2002), peak acceleration

(Algermissen and Perkins, 1976; Khattri et al., 1984; Gupta and Joshi, 2001), peak strain in soils (Todorovska and Trifunac, 1996b), probability of liquefaction (Trifunac and Todorovska, 1999), or the response spectral amplitudes at different natural periods (Lee and Trifunac, 1987; Trifunac, 1988, 1990a). However, the most widely used parameter is the peak ground acceleration. The zoning maps prepared for different parts of the world under the Global Seismic Hazard Analysis Program (GSHAP), which are compiled in a special issue of Annali de Geofisica (December 1999), are also in terms of the peak acceleration. In case of the spectral amplitudes, several zoning maps are required to be prepared for different natural periods and damping ratios, so that the complete spectrum can be constructed by reading the spectral amplitude at each period for a specified damping ratio. In addition, for any of the strong-motion parameters, the zoning maps may be prepared for different confidence levels and exposure periods. To illustrate the application of the PSHA approach to prepare the seismic zoning maps and to highlight the important characteristics of such maps, typical zoning maps in terms of the PSA amplitudes are presented for an area having the geometry and the seismicity similar to that of the Maharashtra state.

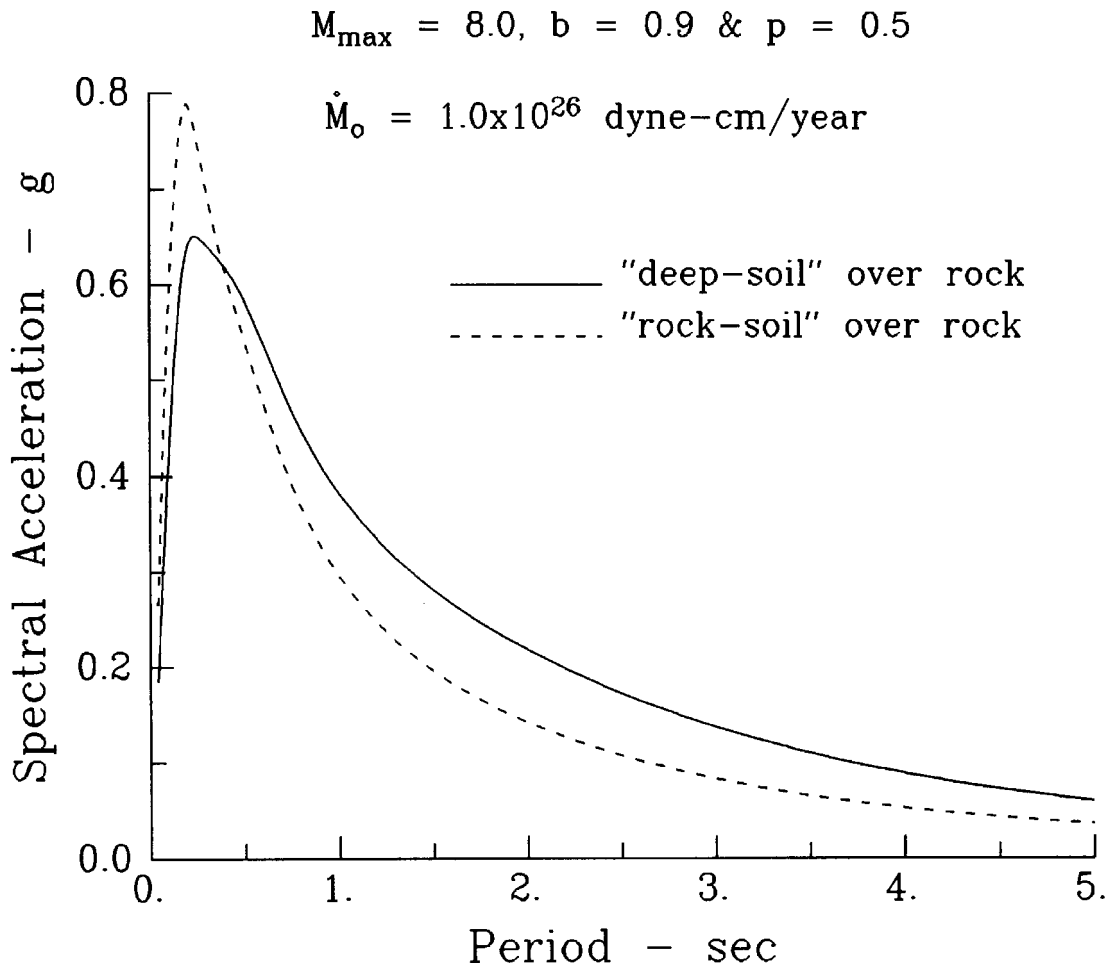

Fig. 10 Illustration of the effect of local soil condition on the uniform hazard response spectra

From a knowledge of the tectonic features and the distribution of the epicenters of available data on past earthquakes, the seismicity of the Maharashtra state and adjoining areas can be defined by twelve (area type) seismic sources with diffused seismicity, as shown in Figure 13 (Gupta et al., 2002). The values of the parameters a and b in the Gutenberg-Richter's relationship and the expected M_{max} for all the seismic sources are taken from Gupta et al. (2002). For the PSHA computations, the seismicity is defined by discretizing the magnitude into seven intervals, with central magnitudes M_j as 3.0, 3.6, 4.2, 4.8, 5.4, 6.0 and 6.6 (with δM_j taken uniformly equal to 0.3 for all the intervals). The exposure period has been considered as 100 years, and the spatial distribution of the total expected seismicity is assumed to be uniform in each of the seismic source areas. To prepare the seismic zoning maps, the entire area of Maharashtra state is defined by a grid of 1728 sites with 0.125^0 latitude and 0.125^0 longitude spacings. Using the contributions from all the earthquakes within 300 km of each of these sites,

PSA amplitudes are computed for four natural periods equal to 0.04, 0.19, 0.9 and 2.8 s, and two confidence levels equal to 0.5 and 0.84. The site soil and the geological conditions are both taken to be as hard rock type for the computation of these results. The zoning maps thus obtained for confidence levels of 0.50 and 0.84 are shown plotted in Figures 14 and 15, respectively. It is seen that in addition to the confidence level, the distribution of seismic hazard changes with the natural period, and hence a single zoning map in terms of peak ground acceleration does not provide a realistic picture of hazard to structures with different natural periods. The maps like those in Figures 14 and 15 are able to consider simultaneously and in a balanced way, the effects of all the parameters like level of seismicity, spatial distribution of seismicity, local soil and geological conditions, and the attenuation characteristics of the strong-motion parameters. The variation in any of these governing parameters is manifested by corresponding changes in the distribution of seismic hazard. The PSHA methodology is also able to consider the uncertainties in the input parameters and the random scattering in the data.

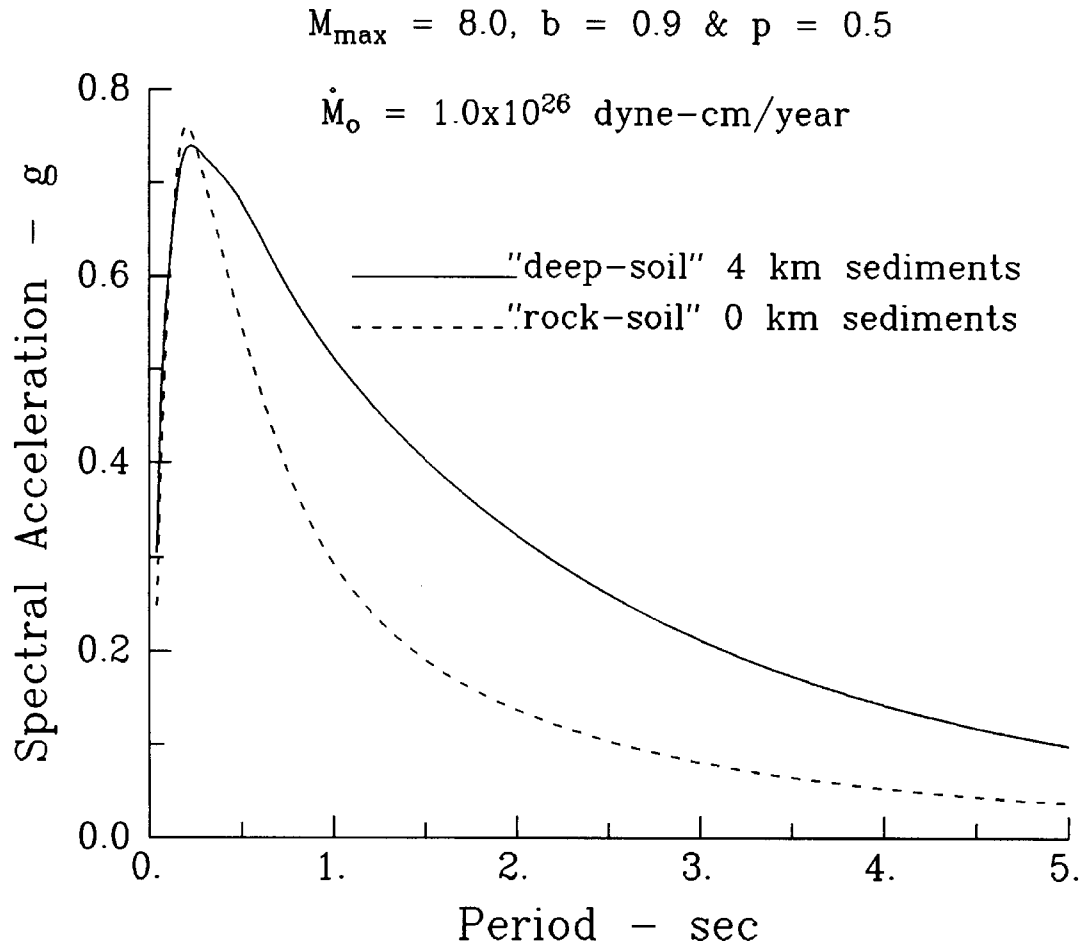

Fig. 11 Comparison of the uniform hazard response spectra for two extreme site conditions defined by hard rock and deep-soil overlying thick sediments

DISCUSSION AND CONCLUSIONS

The present paper has described the current state-of-the-art approaches for the deterministic and the probabilistic seismic hazard analyses. The basic inputs required for both the approaches are the same, which include data on past seismicity, knowledge of the tectonic features, information on site soil condition and the underlying geology of the surrounding area, and the attenuation characteristics of the strong-motion parameter to be used for quantifying the hazard. The first step of analysis is also the same in both the approaches, wherein all possible seismic source zones are identified on the basis of available data on tectonic features and the spatial distribution of the epicenters of past earthquakes. Then, in the deterministic seismic hazard analysis (DSHA), the maximum possible earthquake is estimated for each of the seismic sources. This earthquake, commonly termed as maximum credible earthquake (MCE), is

assumed to occur at a location in the particular seismic source zone, which minimizes its distance from the site of interest. For each of these MCEs, the value of the associated strong-motion parameter at the selected site is most commonly estimated by using an appropriate empirical attenuation relationship. The MCE that produces the largest value of the strong-motion parameter is considered for practical applications, with the conviction that it will never be exceeded.

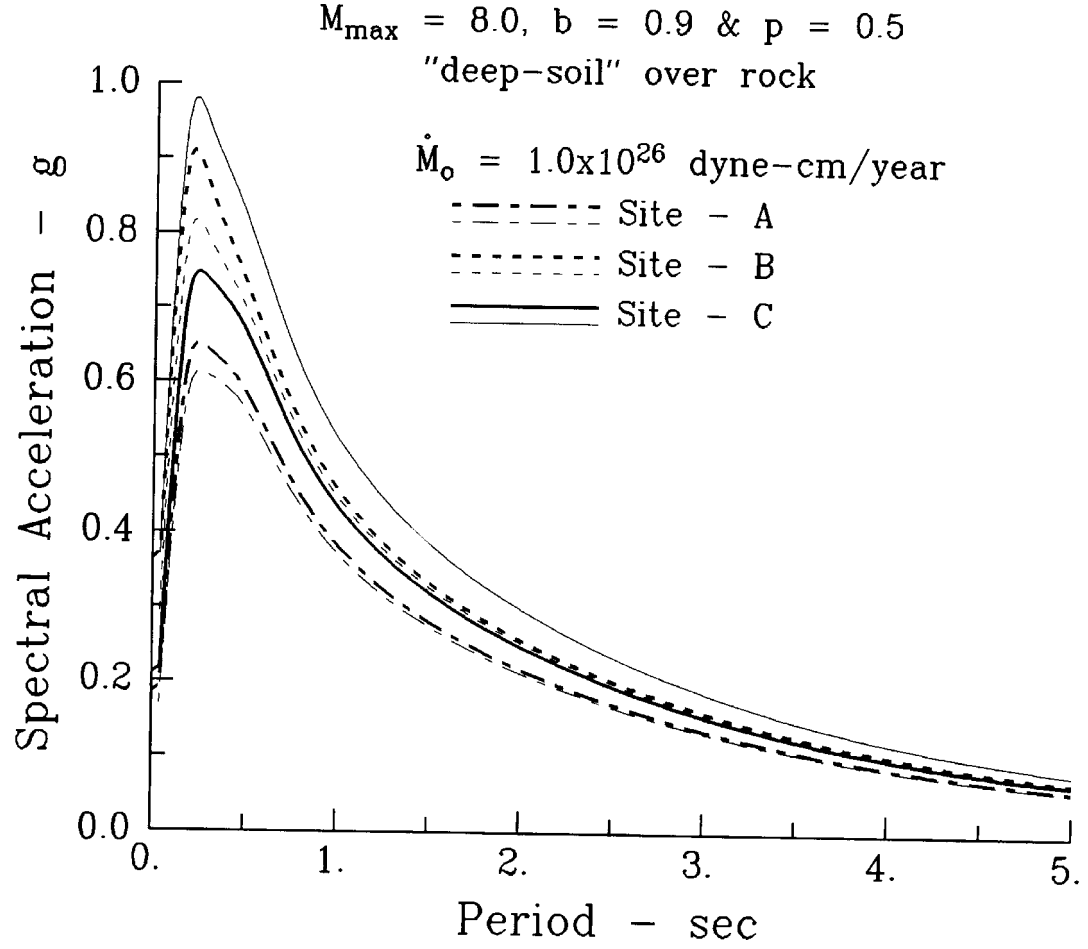

Fig. 12 Illustration of the changes in uniform hazard response spectra with the changes in the spatial distribution of the seismicity (the thick curves correspond to a nonuniform and thin curves to a uniform spatial distribution of the seismicity)

However, the DSHA approach lacks a rational scientific basis and may not always ensure the intended conservatism. The database used and each step of analysis are generally associated with large uncertainties, and thus, selecting the most pessimistic scenario is neither likely to represent reality nor is a good engineering decision. Further, one might be prepared to take at least the same amount of risk in case of earthquakes, to which he is prone in the daily walk of life. However, the DSHA does not provide a means to quantify this risk. In the PSHA approach, the maximum possible earthquake in each seismic source is assigned a finite probability of occurrence during a specified time interval, to account for the fact that the recurrence interval of such an event is normally much longer than the time periods of interest in practical applications. In addition, the total expected numbers of earthquakes with different lower magnitudes during a specified time interval are also considered as per the Gutenberg-Richter's relationship. To account for the random spatial distribution of all these earthquakes for each of the sources, they are distributed appropriately within the entire source zone. Then, a strong-motion parameter of interest is estimated at the selected site with a desired confidence level by defining a composite probability distribution function as a result of the total expected seismicity in all the source zones, with the observed scattering in the strong motion parameter taken into account. Thus, by incorporating the effects of various random uncertainties in the input parameters, the probabilistic seismic hazard analysis (PSHA) approach provides an avenue to arrive at more objective and cost-effective engineering decisions. If desired for some engineering applications, a single pair of magnitude and distance, which can

reproduce the results of the PSHA for a selected site, can also be obtained by de-aggregation of the probabilistic seismic hazard.

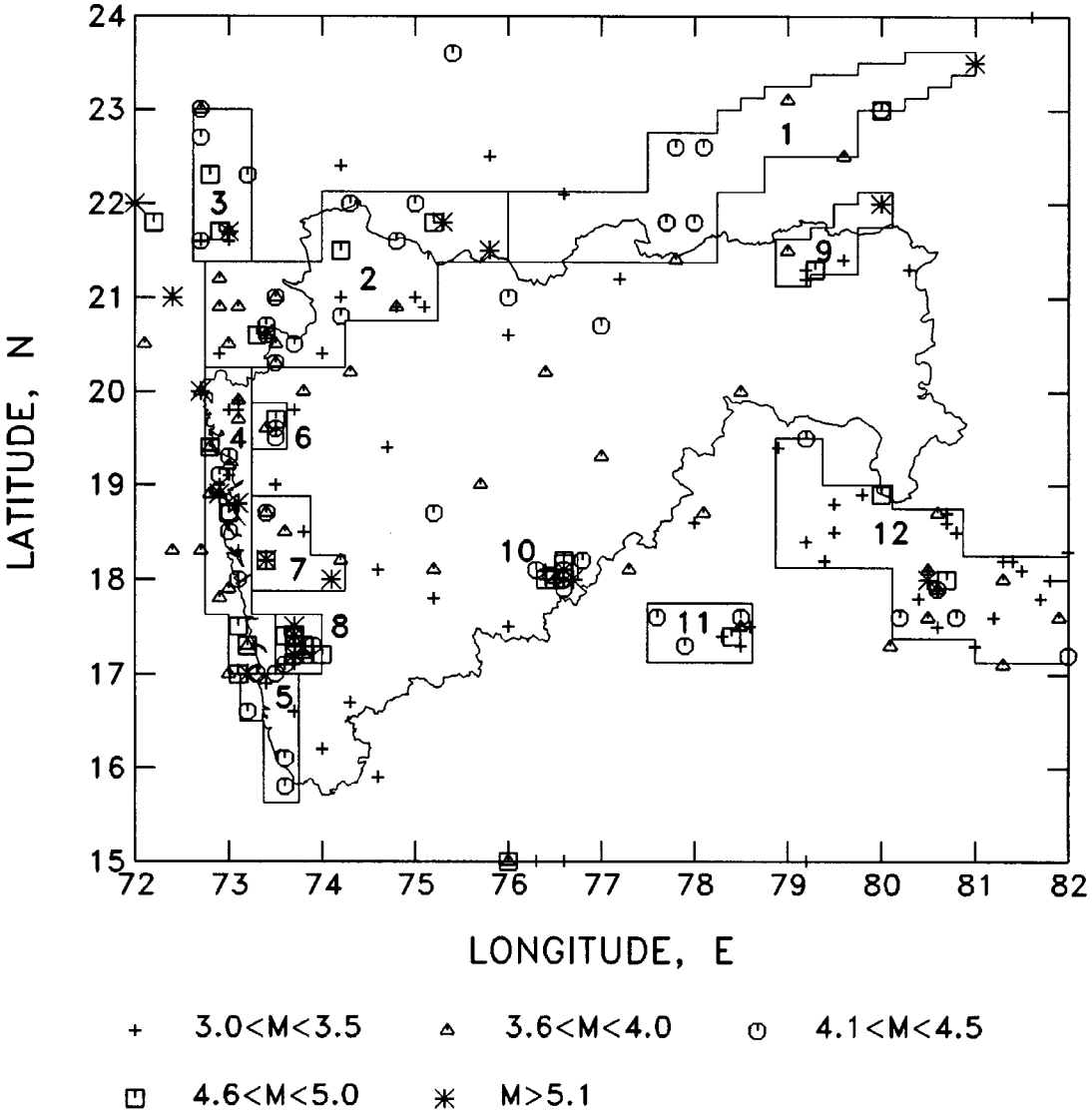

Fig. 13 Twelve possible seismic sources and the distribution of epicenters of available data on past earthquakes in the state of Maharashtra and its adjoining areas

In most of the practical applications, exact knowledge of seismic source geometries, fault rupture scenarios, recurrence model for seismic activity rate, and the attenuation relations for the strong motion parameters is lacking, which makes it difficult to arrive at an unequivocal single representation of seismic sources, their seismicity and the ground motion attenuation. For any particular case, several widely differing and competing alternatives may thus be proposed by different investigators (epistemic uncertainties). As there is no simple way to select the optimum and the most effective alternative, the "mean" or "median" value of the strong motion parameter obtained from several physically plausible models is recommended to be used to get an unbiased estimate of the probabilistic seismic hazard. The DSHA approach can also incorporate the effects of the epistemic uncertainties by computing the mean and median values by considering all possible alternatives regarding the maximum magnitude and its closest distance from a selected site, as well as the ground motion attenuation relation. However, the aleatory uncertainties related to the random nature of the various input parameters are not considered in the deterministic formulation.

Further, it may be noted that the seismic hazard at a site for different frequency ranges is governed by earthquakes with different magnitude and distance combinations. Thus, a single deterministic pair of magnitude and distance is unable to provide the design response spectrum with a desired confidence level for all the natural periods. Also, the results of DSHA approach are, in general, very sensitive to the

choice of the MCE magnitude and its distance, which makes it very difficult to arrive at a stable and reliable estimate. The uniform hazard response spectrum computed by the PSHA approach has the property that with a specified confidence level, it will not be exceeded at any of the periods due to any of the earthquakes expected during a given time interval, thus taking the randomness of earthquake occurrences in space, time and magnitude into account. The paper has also illustrated the use of the PSHA approach to prepare probabilistic seismic zoning maps for the spectral amplitudes at different natural periods with a specified confidence level and a given exposure time. Such maps are able to portray in a balanced way the effects of all the governing factors related to seismicity and the geology on the strong-motion parameter of zoning.

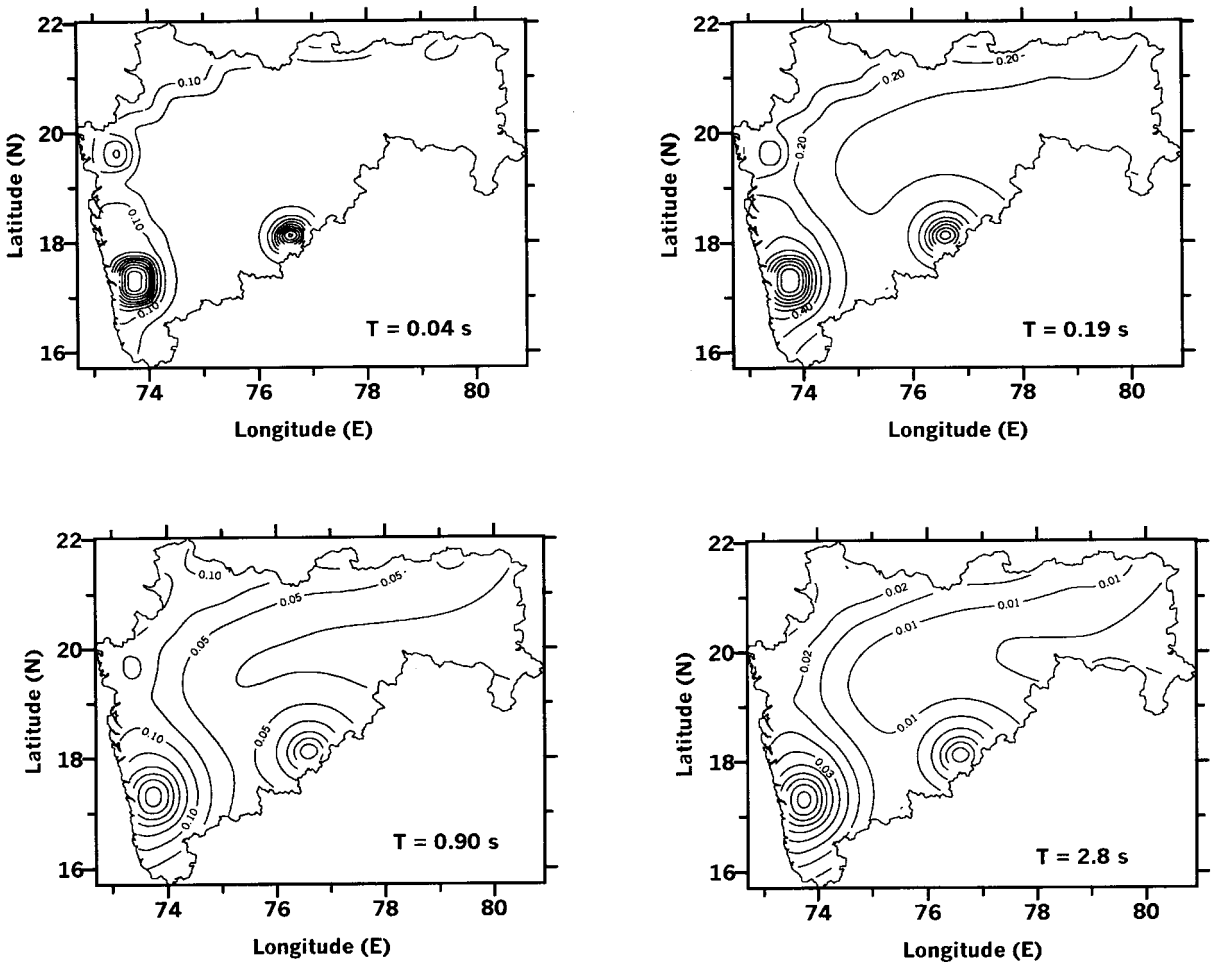

Fig. 14 Seismic zoning maps with a confidence level of 0.50 and exposure time of 100 years for the state of Maharashtra in terms of PSA amplitudes at four natural periods

Though it may be difficult to establish an approach to seismic hazard assessment that will be the ideal tool for all situations (Bommer, 2002), in view of the above discussion, it may be concluded that the PSHA approach should be a preferred choice. Acknowledging the fact that the basic purpose of both DSHA and PSHA approaches is to facilitate engineering designs and decisions, and not to predict the actual earthquakes and ground motions, it is concluded that the PSHA approach provides a scientifically more sound method for seismic hazard analysis.

ACKNOWLEDGEMENTS

The author is grateful to Mrs. V.M. Bendre, Director, Central Water and Power Research Station, Pune for showing very keen interest in the present research work and for according her permission for publication of this paper.

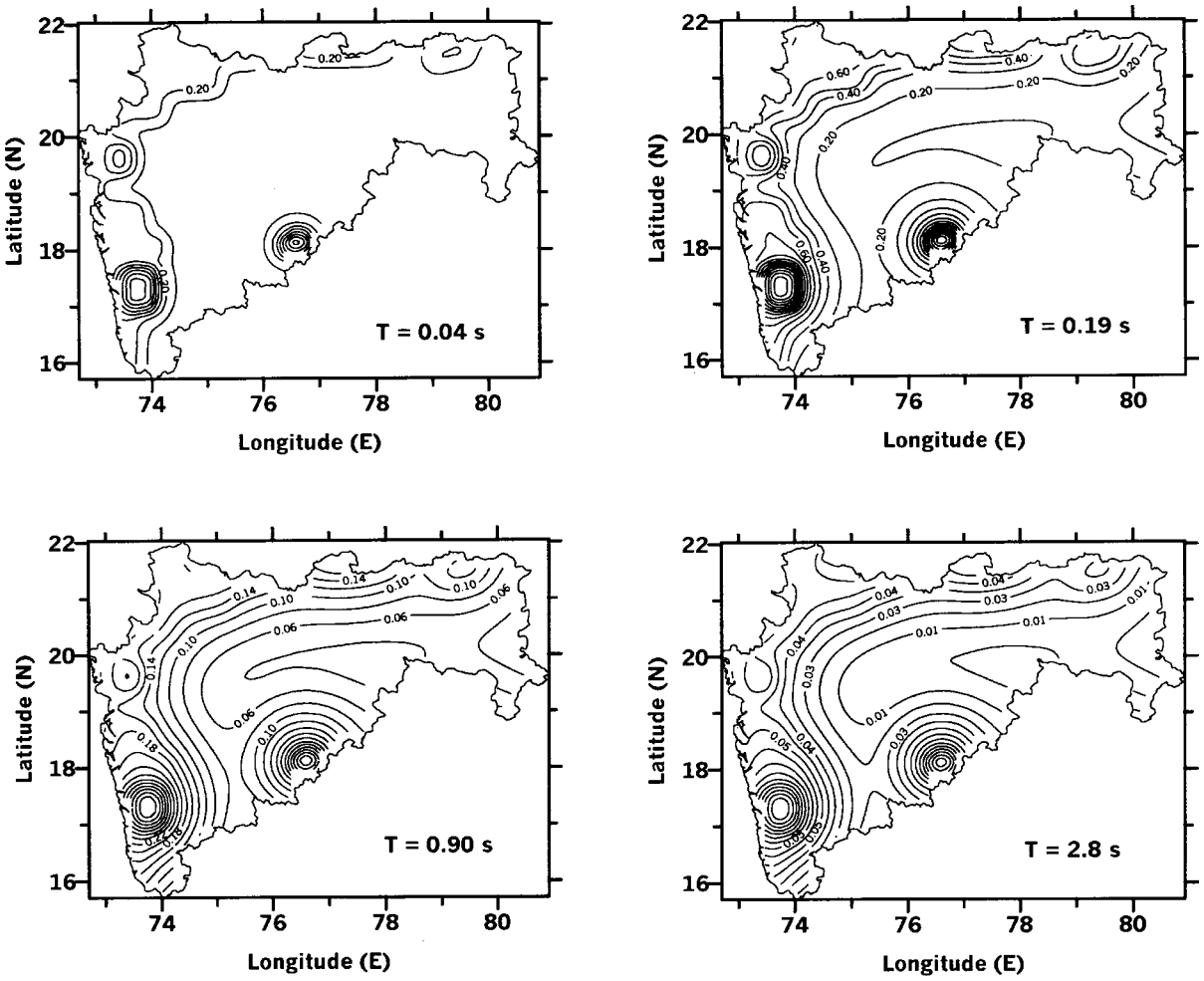

Fig. 15 Seismic zoning maps with a confidence level of 0.84 and exposure time of 100 years for the state of Maharashtra in terms of PSA amplitudes at four natural periods

REFERENCES

1. Abrahamson, N.A. (2000). "Treatment of Variability and Uncertainty in Numerical and Empirical Methods for Ground Motion Estimation", Proc. 2nd US-Japan Workshop on Performance-Based Earthq. Eng. Methodology for Reinforced Concrete Building Structures, Sapporo, Japan, pp. 63-73.
2. Algermissen, S.T. and Perkins, D.M. (1976). "A Probabilistic Estimate of Maximum Acceleration in Rock in the Contiguous United States", Open-File Report 76-416, U.S. Geological Survey.
3. Anderson, J.G. (1978). "On the Attenuation of Modified Mercalli Intensity with Distance in the United States", Bull. Seism. Soc. Am., Vol. 68, pp. 1147-1179.
4. Anderson, J.G. and Luco, J.E. (1983). "Consequence of Slip Rate Constraints on Earthquake Occurrence Relations", Bull. Seism. Soc. Am., Vol. 73, pp. 471-496.
5. Anderson, J.G. and Trifunac, M.D. (1977a). "Uniform Risk Functionals for Characterisation of Strong Earthquake Ground Motion", Report CE 77-02, Dept. of Civil Eng., University of Southern California, Los Angeles, California, U.S.A.
6. Anderson, J.G. and Trifunac, M.D. (1977b). "Uniform Risk Functionals for Characterisation of Strong Earthquake Ground Motion", Proc. Second Annual ASCE EMD Specialty Conference, North Carolina State Univ., Raleigh, N.C., U.S.A., pp. 332-335.
7. Anderson, J.G. and Trifunac, M.D. (1978a). "Uniform Risk Functionals for Characterization of Strong Earthquake Ground Motion", Bull. Seism. Soc. Am., Vol. 68, pp. 205-218.

8. Anderson, J.G. and Trifunac, M.D. (1978b). "Application of Seismic Risk Procedures to Problems in Microzonation", Proc. 2nd Int. Conf. on Microzonation for Safer Construction, Research and Applications, Vol. I, pp. 559-569.
9. Anderson, J.G. and Trifunac, M.D. (1979). "A Note on Probabilistic Computation of Earthquake Response Spectrum Amplitudes", Nuclear Engineering and Design, Vol. 51, pp. 285-294.
10. Anderson, J.G., Lee, V.W. and Trifunac, M.D. (1987). "Methods for Introduction of Geological Data into Characterisation of Active Faults and Seismicity and Upgrading of the Uniform Risk Spectrum Technique", U.S. Nuclear Regulatory Commission, Report NUREG/CR-4903.
11. Bilham, R. and Gaur, V.K. (2000). "Geodetic Contributions to the Study of Seismotectonics in India", Current Science, Vol. 79, pp. 1259-1269.
12. Biot, M.A. (1942). "Analytical and Experimental Methods in Engineering Seismology", ASCE Transactions, Vol. 5, pp. 365-408.
13. Bommer, J.J. (2002). "Deterministic versus Probabilistic Seismic Hazard Assessment: An Exaggerated and Obstructive Dichotomy", Jour. Earthq. Eng., Vol. 6, Special Issue 1, pp. 43-73.
14. Bonilla, M.G. and Buchanon, J.M. (1970). "Interim Report on World-Wide Historic Surface Faulting", Open-File Report 70-34, U.S. Geological Survey.
15. Bonilla, M.G., Markad, R.K. and Lienkaemper, J.J. (1984). "Statistical Relations among Earthquake Magnitude, Surface Rupture Length, and Surface Rupture Displacement", Bull. Seism. Soc. Am., Vol. 74, pp. 2379-2411.
16. Boore, D.M. and Atkinson, B.M. (1987). "Stochastic Prediction of Ground Motion and Spectral Response at Hard-Rock Sites in Eastern North America", Bull. Seism. Soc. Am., Vol. 77, pp. 440-467.
17. Chen, P.S. and Lin, P.H. (1973). "An Application of Theory of Extreme Values to Moderate and Long-Interval Earthquake Prediction", Acta Geophys., Vol. 16, p. 6.
18. Coppersmith, K.J. and Youngs, R.R. (1986). "Capturing Uncertainties in Probabilistic Seismic Hazard Assessments within Intraplate Environments", Proc. 3rd National Conf. on Earthq. Eng., Charleston, South Carolina, U.S.A., Vol. I, pp. 301-312.
19. Cornell, C.A. (1968). "Engineering Seismic Risk Analysis", Bull. Seism. Soc. Am., Vol. 58, No. 5, pp. 1583-1606.
20. David, P.M., Jackson, D.D. and Kagan, Y.Y. (1989). "The Longer It Has Been since the Last Earthquake, the Longer the Expected Time till the Next", Bull. Seism. Soc. Am., Vol. 79, No. 5, pp. 1439-1456.
21. Douglas, J. (2001). "A Comprehensive Worldwide Summary of Strong-Motion Attenuation Relationships for Peak Ground Acceleration and Spectral Ordinates (1969 to 2000)", ESEE Report 01-1, Civil Engineering Dept., Imperial College of Science, Technology and Medicine, London, U.K.
22. Dravinski, M., Trifunac, M.D. and Westermo, B.D. (1980). "Ratios of Uniform Risk Spectrum Amplitudes for Different Probabilities of Exceedance and for Shallow, Random Seismicity Surrounding the Site", Report CE 80-02, Dept. of Civil Eng., Univ. of Southern California, Los Angeles, California, U.S.A.
23. Epstein, B. and Lomnitz, C. (1966). "A Model for Occurrence of Large Earthquakes", Nature, Vol. 211, pp. 954-956.
24. Esteva, L. (1969). "Seismicity Prediction, A Bayesian Approach", Proc. 4th World Conf. Earthq. Eng., Santiago, Chile.
25. Geller, R.J. (1976). "Scaling Relations for Earthquake Source Parameters and Magnitude", Bull. Seism. Soc. Am., Vol. 66, pp. 1501-1523.
26. Gumbel, E.J. (1958). "Statistics of Extremes", Columbia Univ. Press, New York, U.S.A.
27. Gupta, I.D. (1991). "A Note on Computing Uniform Risk Spectra from Intensity Data on Earthquake Occurrence", Soil Dyn. Earthq. Eng., Vol. 10, No. 8, pp. 407-413.
28. Gupta, I.D. (2002). "Should Normalised Spectral Shapes be Used for Estimating Site-Specific Design Ground Motion?", Proc. 12th Symp. on Earthq. Eng., Indian Institute of Technology Roorkee, Roorkee, Vol. I, pp. 168-175.

29. Gupta, I.D. and Deshpande, V.C. (1994). "Application of Log-Pearson Type-3 Distribution for Evaluation of Design Earthquake Magnitude", Jour. Inst. Engineers (India), Civil Div., Vol. 75, pp. 129-134.
30. Gupta, I.D. and Joshi, R.G. (1993). "On Synthesizing Response Spectrum Compatible Accelerograms", European Earthq. Eng., Vol. 7, pp. 25-33.
31. Gupta, I.D. and Joshi, R.G. (1996). "Evaluation of Design Earthquake Ground Motion for Soil and Rock Sites", Proc. Workshop on Design Practices in Earthq. Geotech. Eng., Roorkee, pp. 58-87.
32. Gupta, I.D. and Joshi, R.G. (2001). "Probabilistic Seismic Zoning of Maharashtra State", Proc. Workshop on Seismicity of Western India with Special Reference to Recent Kutch Earthquake, Paper No. 1, Pune.
33. Gupta, I.D. and Rambabu, V. (1996). "Simulation of Design Response Spectra of Strong-Motion Acceleration in Koyna Dam Region Using Seismological Source Model Approach", Bull. Ind. Soc. Earthq. Tech., Vol. 33, No. 2, pp. 181-193.
34. Gupta, I.D. and Trifunac, M.D. (1988). "Attenuation of Intensity with Epicentral Distances in India", Soil Dyn. Earthq. Eng., Vol. 7, pp. 162-169.
35. Gupta, I.D., Joshi, R.G. and Rambabu, V. (2002). "An Example of Seismic Zoning Using PSHA Approach", MAEER's MIT Pune Jour., Vol. IX, No. 1-4, pp. 107-116.
36. Gupta, I.D., Nagle, B.R. and Pagare, V.S. (1988). "An Investigation for the Probabilities of Maximum Earthquake Magnitudes in Northwest Himalayan Region", Bull. Ind. Soc. Earthq. Tech., Vol. 25, pp. 11-22.
37. Gupta, I.D., Joshi, R.G., Rambabu, V. and Rame Gowda, B.M. (1999). "Attenuation of MMI with Distance in Peninsular India", European Earthq. Eng., Vol. 13, pp. 25-32.
38. Gutenberg, B. and Richter, C.F. (1954). "Seismicity of the Earth and Associated Phenomena", Princeton Univ. Press, Princeton, New Jersey, U.S.A.
39. Hadley, D.M. and Helmberger, D.V. (1980). "Simulation of Strong Ground Motions", Bull. Seism. Soc. Am., Vol. 70, pp. 610-617.
40. Hanks, T.C. and Kanamori, H. (1979). "A Moment Magnitude Scale", Jour. Geophys. Res., Vol. 84, pp. 2348-2350.
41. Hartzell, S.H. (1982). "Simulation of Ground Acceleration for May 1980 Mammoth Lakes, California Earthquakes", Bull. Seism. Soc. Am., Vol. 72, pp. 2381-2387.
42. Housner, G.W. (1959). "Behaviour of Structures during Earthquakes", Jour. Eng. Mech. Div., ASCE, Vol. 85, pp. 109-129.
43. IAEE (1984). "Earthquake Resistant Regulations, A World List-1984", International Association of Earthquake Engineering, Gakujutsu Bunken Fukyn-Kai, Tokyo, Japan.
44. Iida, K. (1965). "Earthquake Magnitude, Earthquake Fault, and Source Dimensions", Jour. Earthq. Sci., Nagoya Univ., Vol. 13, pp. 115-132.
45. Irikura, K. and Muramatu, I. (1982). "Synthesis of Strong Ground Motions from Large Earthquakes Using Observed Seismograms of Small Events", Proc. 3rd International Microzonation Conf., Seattle, U.S.A., pp. 447-458.
46. Ishikawa, Y. and Kameda, H. (1988). "Hazard Consistent Magnitude and Distance for Extended Seismic Risk Analysis", Proc. 9th World Conf. Earthq. Eng., Vol. 2, pp. 89-94.
47. Jara, J.M. and Rosenblueth, E. (1988). "Probability Distribution of Times between Characteristic Subduction Earthquakes", Earthq. Spectra, Vol. 4, pp. 449-531.
48. Jordanovski, L.R., Todorovska, M.I. and Trifunac, M.D. (1991). "A Model for Assessment of the Total Loss in a Building Exposed to Earthquake Hazard", Report CE 92-05, Dept. of Civil Eng., Univ. of Southern California, Los Angeles, California, U.S.A.
49. Jordanovski, L.R., Todorovska, M.I. and Trifunac, M.D. (1993). "Total Loss in a Building Exposed to Earthquake Hazard, Part I: The Model; Part II: A Hypothetical Example", European Earthq. Eng., Vol. VI, No. 3, pp. 14-32.
50. Kameda, H. (1994). "Probabilistic Seismic Hazard and Stochastic Ground Motions", Engineering Structures, Vol. 16, pp. 547-557.

51. Khattri, K.N., Rogers, A.M. and Algermissen, S.T. (1984). "A Seismic Hazard Map of India and Adjacent Areas", Tectonophysics, Vol. 108, pp. 93-134.
52. Khattri, K.N., Yu, G., Anderson, J.G., Brune, J.N. and Zeng, Y. (1994). "Seismic Hazard Estimation Using Modelling of Earthquake Strong Ground Motions: A Brief Analysis of 1991 Uttarkashi Earthquake, Himalaya and Prognostication for a Great Earthquake in the Region", Current Science, Vol. 67, No. 5, pp. 343-353.
53. Kijko, A. (1983). "A Modified Form of the First Gumbel Distribution Model for the Occurrence of Large Earthquakes", Acta Geophys., Vol. 31, pp. 27-39.
54. Kijko, A. and Graham, G. (1998). "Parametric-Historic Procedure for Probabilistic Seismic Hazard Analysis, Part I: Estimation of Maximum Regional Magnitude $M_{\max}$", Pure and Applied Geophysics, Vol. 152, pp. 413-442.
55. Kijko, A. and Sellevoll, M.A. (1981). "Triple-Exponential Distribution, A Modified Model for the Occurrence of Large Earthquakes", Bull. Seism. Soc. Am., Vol. 71, pp. 2097-2101.
56. Kijko, A. and Sellevoll, M.A. (1989). "Estimation of Earthquake Hazard Parameters from Incomplete Data Files, Part I: Utilization of Extreme and Complete Catalogues with Different Threshold Magnitudes", Bull. Seism. Soc. Am., Vol. 79, pp. 645-654.
57. Krinitzsky, E.L. (1995). "Deterministic versus Probabilistic Seismic Hazard Analysis for Critical Structures", Int. Jour. Eng. Geol., Vol. 40, pp. 1-7.
58. Lee, V.W. (1987). "Influence of Local Soil and Geologic Site Conditions on Pseudo Relative Velocity Response Spectrum Amplitudes of Recorded Strong Motion Accelerations", Report CE 87-05, Dept. of Civil Eng., Univ. of Southern California, Los Angeles, California, U.S.A.
59. Lee, V.W. (1989). "Empirical Scaling of Pseudo Relative Velocity Spectra of Recorded Strong Earthquake Motion in Terms of Magnitude, and Both Local Soil and Geologic Site Classifications", Earthq. Eng. Eng. Vib., Vol. 9, No. 3, pp. 9-29.
60. Lee, V.W. (1990). "Scaling PSV Spectra in Terms of Site Intensity, and Both Local Soil and Geological Site Classifications", European Earthq. Eng., Vol. IV, No. 1, pp. 3-12.
61. Lee, V.W. (1991). "Correlation of Pseudo Relative Velocity Spectra with Site Intensity, Local Soil Classification and Depth of Sediments", Soil Dyn. Earthq. Eng., Vol. 10, No. 3, pp. 141-151.
62. Lee, V.W. (1992). "On Strong Motion Uniform Risk Functionals Computed from General Probability Distributions of Earthquake Recurrences", Soil Dyn. Earthq. Eng., Vol. 11, pp. 357-367.
63. Lee, V.W. (1993). "Scaling PSV from Earthquake Magnitude, Local Soil and Geological Depth of Sediments", Jour. Geotech. Eng., ASCE, Vol. 119, No. 1, pp. 108-126.
64. Lee, V.W. and Trifunac, M.D. (1985). "Uniform Risk Spectra of Strong Earthquake Ground Motion: NEQRISK", Report CE 85-05, Dept. of Civil Eng., Univ. of Southern California, Los Angeles, California, U.S.A.
65. Lee, V.W. and Trifunac, M.D. (1987). "Microzonation of a Metropolitan Area", Report CE 87-02, Dept. of Civil Eng., Univ. of Southern California, Los Angeles, California, U.S.A.
66. Lee, V.W. and Trifunac, M.D. (1989). "A Note on Filtering Strong Motion Accelerograms to Produce Response Spectra of Specified Shape and Amplitude", European Earthquake Eng., Vol. VIII, No. 2, pp. 38-45.
67. Mark, R.K. (1977). "Application of Linear Statistical Model of Earthquake Magnitude versus Fault Length in Estimating Maximum Expectable Earthquakes", Geology, Vol. 5, pp. 464-466.
68. McGuire, R.K. (1995). "Probabilistic Seismic Hazard Analysis and Design Earthquakes: Closing the Loop", Bull. Seism. Soc. Am., Vol. 85, pp. 1275-1284.
69. Mohraz, B. (1976). "A Study of Earthquake Response Spectra for Different Geological Conditions", Bull. Seism. Soc. Am., Vol. 66, pp. 915-935.
70. Newmark, N.M. and Hall, W.J. (1969). "Seismic Design Criteria for Nuclear Reactor Facilities", Proc. 4th World Conf. Earthq. Eng., Vol. B-4, pp. 37-50.
71. Nishenko, S.P. and Buland, R.A. (1987). "A Generic Recurrence Time Distribution for Earthquake Forecasting", Bull. Seism. Soc. Am., Vol. 77, pp. 1382-1399.

72. Nordquist, J.M. (1945). "Theory of Largest Values Applied to Earthquake Magnitudes", Trans. Am. Geophys. Union, Vol. 26, pp. 29-31.

73. Papastamatiou, D. (1980). "Incorporation of Crustal Deformation to Seismic Hazard Analysis", Bull. Seism. Soc. Am., Vol. 70, pp. 1323-1335.

74. Romeo, R. and Prestininzi, A. (2000). "Probabilistic versus Deterministic Seismic Hazard Analysis: An Integrated Approach for Siting Problems", Soil Dyn. Earthq. Eng., Vol. 20, pp. 75-84.

75. Savy, J.B., Foxall, W., Abrahamson, N. and Bernreuter, D. (2002). "Guidance for Performing Probabilistic Seismic Hazard Analysis for a Nuclear Plant Site: Example Application to the Southeastern United States", Report NUREG/CR-6607, U.S. Nuclear Regulatory Commission, Washington, D.C., U.S.A.

76. Scholz, C.H. (1968). "The Frequency-Magnitude Relation of Microfracturing in Rock and its Relation to Earthquakes", Bull. Seism. Soc. Am., Vol. 58, pp. 399-415.

77. Schwartz, D.P. and Coppersmith, K.J. (1984). "Fault Behavior and Characteristic Earthquakes: Examples from the Wasatch and San Andreas Faults", J. Geophys. Res., Vol. 89, pp. 5681-5698.

78. Seeber, L. and Armbruster, J.G. (1981). "Great Detachment Earthquakes along the Himalayan Arc and Long Term Forecasting", in "Earthquake Prediction - An International Review", Maurice Ewing Series 4, Am. Geophys. Union, Washington, D.C., U.S.A., pp. 259-277.

79. Seed, H.B., Ugas, C. and Lysmer, J. (1976). "Site-Dependent Spectra for Earthquake Resistant Design", Bull. Seism. Soc. Am., Vol. 66, pp. 221-243.

80. Singh, S.K., Bazan, E. and Esteva, L. (1980). "Expected Earthquake Magnitude from a Fault", Bull. Seism. Soc. Am., Vol. 70, pp. 903-914.

81. Smith, S.W. (1976). "Determination of Maximum Earthquake Magnitude", Geophys. Res. Letters, Vol. 33, pp. 351-354.

82. SSHAC (1997). "Recommendations for Probabilistic Seismic Hazard Analysis: Guidance on Uncertainty and Use of Experts", Report NUREG/CR-6372, Senior Seismic Hazard Analysis Committee, U.S. Nuclear Regulatory Commission, Washington, D.C., U.S.A.

83. Stepp, J.C. (1973). "Analysis of Completeness of the Earthquake Sample in the Puget Sound Area", in "Seismic Zoning (edited by S.T. Harding)", NOAA Tech. Report ERL 267-ESL30, Boulder, Colorado, U.S.A.

84. Stepp, J.C. and Wong, I.G. (2001). "Probabilistic Seismic Hazard Analyses for Ground Motions and Fault Displacement at Yucca Mountain, Nevada", Earthquake Spectra, Vol. 17, No. 1, pp. 113-151.

85. Todorovska, M.I. (1994). "Comparison of Response Spectrum Amplitudes from Earthquakes with Lognormally and Exponentially Distributed Return Periods", Soil Dyn. Earthq. Eng., Vol. 13, pp. 97-116.

86. Todorovska, M.I. and Trifunac, M.D. (1996a). "A Seismic Hazard Model for Peak Strains in Soils during Strong Earthquake Shaking", Earthq. Eng. Eng. Vib., Vol. 16, Supplement, pp. 1-12.

87. Todorovska, M.I. and Trifunac, M.D. (1996b). "Hazard Mapping of Normalized Peak Strain in Soil during Earthquakes - Microzonation of a Metropolitan Area", Soil Dyn. Earthq. Eng., Vol. 15, No. 5, pp. 321-329.

88. Todorovska, M.I. and Trifunac, M.D. (1999). "Liquefaction Opportunity Mapping via Seismic Wave Energy", Jour. Geotech. Geoenvironmental Eng., ASCE, Vol. 125, No. 12, pp. 1032-1042.

89. Todorovska, M.I., Gupta, I.D., Gupta, V.K., Lee, V.W. and Trifunac, M.D. (1995). "Selected Topics in Probabilistic Seismic Hazard Analysis", Report CE 95-08, Dept. of Civil Eng., Univ. of Southern California, Los Angeles, California, U.S.A.

90. Tocher, D. (1958). "Earthquake Energy and Ground Breakage", Bull. Seism. Soc. Am., Vol. 48, pp. 147-153.

91. Trifunac, M.D. (1970). "On the Statistics and Possible Triggering Mechanism of Earthquakes in Southern California", Report EERL 70-03, Earthquake Eng. Research Lab., Calif. Inst. of Technology, Pasadena, California, U.S.A.

92. Trifunac, M.D. (1976). "Preliminary Empirical Model for Scaling Fourier Amplitude Spectra of Strong Ground Acceleration in Terms of Earthquake Magnitude, Source to Station Distance and Recording Site Conditions", Bull. Seism. Soc. Am., Vol. 66, pp. 1345-1373.
93. Trifunac, M.D. (1977). "Uniformly Processed Strong Earthquake Ground Accelerations in the Western United States of America for the Period from 1933 to 1971: Pseudo Relative Velocity Spectra and Processing Noise", Report CE 77-04, Dept. of Civil Eng., Univ. of Southern California, Los Angeles, California, U.S.A.
94. Trifunac, M.D. (1979). "Preliminary Empirical Model for Scaling Fourier Amplitude Spectra of Strong Motion Acceleration in Terms of Modified Mercalli Intensity and Geological Site Condition", Earthq. Eng. Struct. Dyn., Vol. 7, pp. 63-74.
95. Trifunac, M.D. (1987). "Influence of Local Soil and Geologic Site Conditions on Fourier Spectrum Amplitudes of Recorded Strong Motion Accelerations", Report CE 87-04, Dept. of Civil Eng., Univ. of Southern California, Los Angeles, California, U.S.A.
96. Trifunac, M.D. (1988). "Seismic Microzonation Mapping via Uniform Risk Spectra", Proc. 9th World Conf. Earthq. Eng., Vol. VII, pp. 75-80.
97. Trifunac, M.D. (1989a). "Seismic Microzonation", Proc. UNDRO Seminar on Lessons Learned from Earthquakes, Moscow, USSR, pp. 21-27.
98. Trifunac, M.D. (1989b). "Threshold Magnitudes Which Cause Ground Motion Exceeding the Values Expected during the Next 50 Years in a Metropolitan Area", Geofizika, Vol. 6, pp. 1-12.
99. Trifunac, M.D. (1989c). "Dependence of Fourier Spectrum Amplitudes of Recorded Strong Earthquake Accelerations on Magnitude, Local Soil Conditions and on Depth of Sediments", Earthq. Eng. Struct. Dyn., Vol. 18, pp. 999-1016.
100. Trifunac, M.D. (1989d). "Empirical Scaling of Fourier Spectrum Amplitudes of Recorded Strong Earthquake Accelerations in Terms of Magnitude and Local Soil and Geologic Conditions", Earthq. Eng. Eng. Vib., Vol. 9, No. 2, pp. 23-44.
101. Trifunac, M.D. (1990a). "A Microzonation Method Based on Uniform Risk Spectra", Soil Dyn. Earthq. Eng, Vol. 9, No. 1, pp. 34-43.
102. Trifunac, M.D. (1990b). "How to Model Amplification of Strong Earthquake Motions by Local Soil and Geologic Site Conditions", Earthq. Eng. Struct. Dyn., Vol. 19, No. 6, pp. 833-846.
103. Trifunac, M.D. (1991). "Empirical Scaling of Fourier Spectrum Amplitudes of Recorded Strong Earthquake Accelerations in Terms of Modified Mercalli Intensity, Local Soil Conditions and Depth of Sediments", Soil Dyn. Earthq. Eng., Vol. 10, No. 1, pp. 65-72.
104. Trifunac, M.D. (1992). "Should Peak Acceleration be Used to Scale Design Spectrum Amplitudes?", Proc. 10th World Conf. on Earthq. Eng., Madrid, Spain, Vol. 10, pp. 5817-5822.
105. Trifunac, M.D. (1993). "Broad Band Extension of Fourier Amplitude Spectra of Strong Motion Acceleration", Report CE 93-01, Dept. of Civil Eng., Univ. of Southern California, Los Angeles, California, U.S.A.
106. Trifunac, M.D. (1994). "Similarity of Strong Motion Earthquakes in California", European Earthquake Eng., Vol. VIII, No. 1, pp. 38-48.
107. Trifunac, M.D. (1998). "Stresses and Intermediate Frequencies of Strong Motion Acceleration", Geofizika, Vol. 14, pp. 1-27.
108. Trifunac, M.D. and Anderson, J.G. (1977). "Preliminary Empirical Models for Scaling Absolute Acceleration Spectra", Report CE 77-03, Dept. of Civil Eng., Univ. of Southern California, Los Angeles, California, U.S.A.
109. Trifunac, M.D. and Anderson, J.G. (1978a). "Preliminary Empirical Models for Scaling Pseudo Relative Velocity Spectra", Report CE 78-04, Dept. of Civil Eng., Univ. of Southern California, Los Angeles, California, U.S.A.
110. Trifunac, M.D. and Anderson, J.G. (1978b). "Preliminary Models for Scaling Relative Velocity Spectra", Report CE 78-05, Dept. of Civil Eng., Univ. of Southern California, Los Angeles, California, U.S.A.

111. Trifunac, M.D. and Lee, V.W. (1978). "Dependence of Fourier Amplitude Spectra of Strong Motion Acceleration on the Depth of Sedimentary Deposits", Report CE 78-14, Dept. of Civil Eng., Univ. of Southern California, Los Angeles, California, U.S.A.

112. Trifunac, M.D. and Lee, V.W. (1979). "Dependence of Pseudo Relative Velocity Spectra of Strong Motion Acceleration on the Depth of Sedimentary Deposits", Report CE 79-02, Dept. of Civil Eng., Univ. of Southern California, Los Angeles, California, U.S.A.

113. Trifunac, M.D. and Lee, V.W. (1985a). "Frequency Dependent Attenuation of Strong Earthquake Ground Motion", Report CE 85-02, Dept. of Civil Eng., Univ. of Southern California, Los Angeles, California, U.S.A.

114. Trifunac, M.D. and Lee, V.W. (1985b). "Preliminary Empirical Model for Scaling Fourier Amplitude Spectra of Strong Ground Acceleration in Terms of Earthquake Magnitude, Source to Station Distance, Site Intensity and Recording Site Conditions", Report CE 85-03, Dept. of Civil Eng., Univ. of Southern California, Los Angeles, California, U.S.A.

115. Trifunac, M.D. and Lee, V.W. (1985c). "Preliminary Empirical Model for Scaling Pseudo Relative Velocity Spectra of Strong Earthquake Acceleration in Terms of Magnitude, Distance, Site Intensity and Recording Site Conditions", Report CE 85-04, Dept. of Civil Eng., Univ. of Southern California, Los Angeles, California, U.S.A.

116. Trifunac, M.D. and Lee, V.W. (1990). "Frequency Dependent Attenuation of Strong Earthquake Ground Motion", Soil Dyn. Earthq. Eng, Vol. 9, No. 1, pp. 3-15.

117. Trifunac, M.D. and Todorovska, M.I. (1989). "Attenuation of Seismic Intensity in Albania and Yugoslavia", Earthq. Eng. Struct. Dyn., Vol. 18, pp. 617-631.

118. Trifunac, M.D. and Todorovska, M.I. (1998). "Comment on the Role of Earthquake Hazard Maps in Loss Estimation: A Study of the Northridge Earthquake", Earthq. Spectra, Vol. 14, No. 3, pp. 557-563.

119. Tsai, N.C. (1972). "Spectrum Compatible Motions for Design Purposes", Jour. Eng. Mech. Div., ASCE, Vol. 98, pp. 345-356.

120. Utsu, T. (1961). "A Statistical Study on the Occurrence of Aftershocks", Geophys. Mag., Vol. 30, pp. 521-605.

121. Wells, D.L. and Coppersmith, K.J. (1994). "New Empirical Relationships among Magnitude, Rupture Length, Rupture Width, Rupture Area, and Surface Displacement", Bull. Seism. Soc. Am., Vol. 84, pp. 974-1002.

122. Wesnousky, S.G. (1986). "Earthquakes, Quaternary Faults and Seismic Hazard in California", Jour. Geophys. Res., Vol. 91, pp. 12587-12631.

123. Wesnousky, S.G. (1994). "The Gutenberg-Richter or Characteristic Earthquake Distribution, Which Is It?", Bull. Seism. Soc. Am., Vol. 84, No. 6, pp. 1940-1959.

124. Westermo, B.D., Anderson, J.G., Trifunac, M.D. and Dravinski, M. (1980). "Seismic Risk Tables for Pseudo Relative Velocity Spectra in Regions with Shallow Seismicity", Report CE 80-01, Dept. of Civil Eng., Univ. of Southern California, Los Angeles, California, U.S.A.

125. Wong, H.L. and Trifunac, M.D. (1979). "Generation of Artificial Strong Motion Accelerograms", Earthq. Eng. Struct. Dyn., Vol. 7, pp. 509-527.

126. Wyss, M. (1979). "Estimating Maximum Expected Magnitude of Earthquakes from Fault Dimensions", Geology, Vol. 7, pp. 336-340.

127. Wyss, M. and Brune, J.N. (1968). "Seismic Moment, Stress, and Source Dimensions for Earthquakes in the California-Nevada Region", Jour. Geophys. Res., Vol. 73, pp. 4681-4694.

128. Yonekura, N. (1972). "A Review on Seismic Crustal Deformations in and near Japan", Bull. Dept. Geography, Univ. of Tokyo, Vol. 4, pp. 17-50.

129. Youngs, R.R. and Coppersmith, K.J. (1985). "Implications of Fault Slip Rates and Earthquake Recurrence Models to Probabilistic Seismic Hazard Estimates", Bull. Seism. Soc. Am., Vol. 75, No. 4, pp. 939-964.